energies

MDPI

Article

Impact of Triplen Harmonics Generated by Modern Non-Linear Loads on Neutral Conductor Overheating in Low-Voltage Smart Buildings

Teodora Lazar [1], Daria Ionescu [2], Dan Cristian Lazar [1], Florin Gabriel Popescu [1], Adina Milena Tatar [3], Georgeta Buica [4] and Dragos Pasculescu [1,*]

[1] Automation, Computer, Electrical and Power Department, University of Petrosani, 332006 Petrosani, Romania; teodoralazar@upet.ro (T.L.); dan-cristianlazar@upet.ro (D.C.L.); floringpopescu@upet.ro (F.G.P.)
[2] Industrial Engineering and Management Department, University of Petrosani, 332006 Petrosani, Romania; daria.ionescu20@yahoo.com
[3] Department of Industrial and Automation Engineering, University "Constantin Brancusi" of Targu-Jiu, 210135 Targu-Jiu, Romania; adynatatar@gmail.com
[4] Electrical and Mechanical Risks Laboratory, INCDPM "Alexandru Darabont", 35A Blvd Ghencea, 6th County, 062692 Bucharest, Romania; gbuica@protectiamuncii.ro
* Correspondence: dragospasculescu@upet.ro

Abstract

The rapid proliferation of single-phase non-linear loads, such as LED lighting and IT equipment, in modern Smart Buildings has introduced significant power quality challenges in low-voltage electrical installations. A critical but often underestimated consequence is the severe overloading of the neutral conductor caused by triplen harmonics (particularly the 3rd harmonic), which sum algebraically even in balanced three-phase systems. This paper analyzes the electrical and thermal impact of these distortions using a detailed MATLAB/Simulink model of a 400/230 V (3P + N) network. The simulation results demonstrate that under highly distorted conditions (Scenario S3), the neutral current can reach 180% of the nominal phase current (18 A vs. 10 A). Furthermore, the Joule losses analysis reveals a thermal stress more than three times higher on the neutral conductor (peak ~65 W) compared to the phase conductor (~20 W), challenging the traditional design practice of neutral undersizing. To address these safety issues, this study proposes a novel neutral-to-phase current ratio index (k_N) and a proactive decision matrix for Building Management Systems (BMS). Unlike traditional mitigation strategies that rely on static hardware oversizing, passive filters, or specialized transformers, the proposed approach offers a dynamic, cost-effective, and software-driven solution that can be easily integrated into the existing automation infrastructure of modern Smart Buildings. The model identifies a critical tipping point at a 3rd harmonic content of 35.3%, where $k_N \geq 1$. By continuously monitoring the k_N parameter, the proposed algorithm enables a transition from passive protection to active power management, triggering automated responses to prevent insulation degradation and mitigate fire hazards.

Keywords: power quality; non-linear loads; harmonics; modern electric installations; power quality monitoring; neutral conductor overheating; Building Management System (BMS); energy efficiency

Check for updates

Academic Editor: José Matas

Received: 18 March 2026
Revised: 24 March 2026
Accepted: 31 March 2026
Published: 2 April 2026

Copyright: © 2026 by the authors. Licensee MDPI, Basel, Switzerland. This article is an open access article distributed under the terms and conditions of the Creative Commons Attribution (CC BY) license.

1. Introduction

Over the past two decades, the structure of electrical loads in modern buildings has undergone significant transformations, driven by the rapid development of power electronics technologies and the increasing level of automation. LED lighting, IT equipment, intelligent control systems, switched-mode power supplies (SMPS), and general-purpose electronic devices have become dominant in the consumption profile of residential and commercial buildings. Unlike traditional, predominantly linear loads, these devices exhibit a non-linear behavior, drawing non-sinusoidal currents even when supplied by an ideal sinusoidal voltage source.

The increasing share of non-linear loads has led to a progressive deterioration of power quality in low-voltage networks, manifested by the emergence of current harmonics, voltage distortions, and increased electrical power losses [1]. A particularly important aspect is represented by harmonics that are multiples of three, known in the literature as triplen harmonics, which exhibit different properties compared to standard higher-order harmonics. In three-phase systems supplying distributed single-phase loads, these harmonic components are in-phase across all three phase conductors and sum algebraically in the neutral conductor, generating high root-mean-square (RMS) currents.

In low-voltage three-phase installations, the neutral conductor serves to provide the voltage reference and to carry the unbalance currents between phases. Under classical design assumptions, which are based on predominantly linear and balanced loads, the current in the neutral conductor is considered low or even zero. This premise has frequently led to its undersizing or to the use of a common neutral conductor for multiple circuits. In the current context, characterized by the massive presence of non-linear loads, these assumptions are no longer fully valid, and the neutral conductor can become the most electrically and thermally stressed component within the installation.

The motivation behind this paper is to analyze, within a contemporary context, the impact of triplen harmonics generated by modern non-linear loads on the neutral conductor stress in low-voltage Smart Buildings [2]. The main objective of the study is to evaluate the neutral conductor current, the associated harmonic content, and the resulting thermal effects, using a detailed model developed in the MATLAB/Simulink R2022a environment. By correlating the obtained results with the sizing criteria stipulated in international standards, this paper aims to highlight the limitations of classical design approaches and provide useful guidelines for the safe and reliable sizing of the neutral conductor in modern electrical installations. Recent studies [3,4] have intensely analyzed the impact of LED lighting and modern IT equipment on power quality in low-voltage grids. Furthermore, authors in [5,6] highlighted the thermal stress and efficiency degradation in distribution transformers and power systems caused by severe harmonic distortion. However, most existing literature focuses on passive hardware-based mitigation, such as specialized transformers or static conductor oversizing, which often lack the flexibility to adapt to the dynamically changing load profiles of modern installations. There remains a significant gap in comprehensive analyses focusing specifically on the neutral conductor overloading and the arithmetic summation of triplen harmonics within the dual context of contemporary Smart Buildings and older, repurposed facilities. This paper addresses this research gap by shifting the paradigm toward a proactive, software-driven Building Management System (BMS) integration. By introducing the k_N index (neutral-to-phase current ratio) as a real-time control parameter, this study proposes a dynamic safety framework capable of identifying critical tipping points—such as the 180% neutral current accumulation demonstrated in our simulations—ensuring infrastructure integrity before thermal degradation becomes irreversible.

In the current literature, the mitigation of triplen harmonics and neutral conductor overloading is predominantly addressed through hardware-intensive solutions. Existing methods include the deployment of passive and active harmonic filters [1,2], the use of Delta-Wye or Zig-Zag isolation transformers, or the traditional practice of neutral conductor oversizing. While effective at the design stage, these conventional approaches present significant limitations in modern Smart Buildings: they are static, entail high capital costs, and lack the flexibility to adapt to the dynamically changing profile of non-linear loads (e.g., frequent tenant changes or IT infrastructure upgrades). Furthermore, the literature lacks a proactive, software-based diagnostic tool capable of translating real-time power quality indices into automated safety protocols.

To bridge this gap, this paper shifts the paradigm from passive hardware mitigation to active, software-driven Building Management System (BMS) integration.

The main contributions of this paper are summarized as follows:

- The development of a comprehensive MATLAB/Simulink R2022a model to isolate and evaluate the impact of multiple-of-three (triplen) harmonics on the neutral conductor.
- The quantitative demonstration of the thermal stress imbalance (Joule losses) between the phase conductors and the neutral conductor under highly distorted conditions.
- The proposal of the neutral-to-phase current ratio (k_N) as a novel indicator for power quality assessment. While the mathematical ratio of neutral-to-phase current is a known theoretical concept, this study innovates by repurposing the k_N index as a dynamic, real-time control parameter within a proactive BMS architecture.
- The design of a proactive decision matrix for Building Management Systems (BMS), aimed at mitigating fire risks and improving energy efficiency.

2. Triplen Harmonics and Neutral Conductor Stress

2.1. Classification of Current Harmonics and Applied Indices

In modern low-voltage installations, the increasing share of non-linear loads (e.g., switched-mode power supplies, single-phase rectifiers with DC-link capacitors, LED drivers, IT equipment, and electric vehicle chargers) leads to the drawing of non-sinusoidal currents, even when the supply voltage remains generally close to an ideal sinusoidal waveform [7].

To fully understand the impact of these non-linear loads, the influence of the third harmonic on power quality must be justified both theoretically and practically.

- Theoretical Justification: In a balanced three-phase, four-wire system, the fundamental frequency currents are displaced by 120° and vectorially cancel each other out in the neutral conductor. However, the third harmonic and its odd multiples (triplen harmonics) are zero-sequence components. This means their waveforms are completely in phase across all three phases (3 × 50 Hz = 150 Hz). Consequently, instead of canceling out, they add up algebraically in the neutral return path ($I_N = 3 \times I_{3rd}$).
- Practical Justification: From a practical power quality perspective, this mathematical phenomenon has severe consequences. The massive accumulation of current in the neutral conductor causes excessive Joule heating, accelerating insulation degradation and creating significant fire risks, especially since the neutral wire is often unprotected by standard circuit breakers. Furthermore, these high harmonic currents flow through the system's impedance, causing non-sinusoidal voltage drops. This leads to voltage waveform distortion (such as flat-topping) at the load terminals, significantly degrading the power quality delivered to sensitive equipment.

Under these conditions, the line current becomes a distorted periodic waveform, and its analysis requires harmonic decomposition to evaluate the impact on power losses,

the thermal stress of the conductors, and the overall performance of the installation. A non-sinusoidal periodic current can be represented by a Fourier series expansion:

$$i(t) = \sum_{h=1}^{\infty} \sqrt{2}\, I_h \sin(h\omega t + \varphi_h) \quad (1)$$

where I_{h} represents the (RMS) value of the h-th order harmonic, ω is the fundamental angular frequency, and φ_h is the initial phase angle of the respective harmonic component.

From an energy perspective, each harmonic contributes to the total RMS value of the current and, consequently, to the Joule losses in conductors and contacts.

To quantify the overall degree of distortion, the Total Harmonic Distortion of the current (THD_{i}) is used:

$$THD_i = \frac{\sqrt{\sum_{h=2}^{\infty} I_h^2}}{I_1} \quad (2)$$

where THDi is the Total Harmonic Distortion of the current, I_1 is the RMS value of the fundamental component, and I_{h} represents the RMS value of the h-th order harmonic.

The THD_{i} index provides a synthetic measure of the current's "harmonic pollution"; however, it does not fully capture the specific risk associated with the neutral conductor in 3P + N networks. This is because the impact on the neutral conductor depends not only on the magnitudes of the harmonics but also on the phase relationships among the three phases—specifically, how the harmonic components compensate each other or accumulate at the neutral point [8].

In this context, harmonics are grouped into two categories relevant for neutral conductor analysis:

Non-triplen harmonics, with orders that are not multiples of three (e.g., $h \neq 3k$, such as 5, 7, 11, 13), which in a symmetrical three-phase mode have phase shifts of $\pm 120^{\circ}$ and tend to partially cancel out in the sum of the phase currents;

Triplen harmonics, with orders that are multiples of three (e.g., $h = 3k$, such as 3, 9, 15), associated with the zero-sequence, which are in-phase across all three phases and tend to add arithmetically in the neutral conductor.

Therefore, in addition to the global THD_{I} index, this paper explicitly investigates the role of the 3rd-order harmonic, as it is typically the dominant component of the triplen family in modern buildings supplied by single-phase non-linear loads. The share of the third harmonic is expressed by the following index:

$$H_3 = 100 \cdot \frac{I_3}{I_1} \quad (3)$$

which provides a direct measure of the third harmonic's intensity relative to the fundamental component, where H_3 represents the 3rd harmonic content expressed as a percentage, and I_3 is the RMS value of the 3rd-order harmonic current.

The classification of relevant harmonics and their effect on the neutral conductor in a 3P + N system are summarized in Table 1. As can be observed, the risk of neutral overloading is determined not only by the global distortion level (THD_{I}), but particularly by the presence of triplen harmonics (H_3), associated with the zero-sequence. Unlike the fundamental component and non-triplen harmonics, which tend to partially or totally cancel out in a symmetrical mode, triplen harmonics add arithmetically in the neutral conductor.

Thus, an increase in H_3 leads to disproportionate increases in the neutral current, even when the loads are apparently balanced across the phases in terms of RMS values. This fundamental property justifies the methodology of this paper, which consists of correlating

the specific outputs, such as I_N and k_N, with the dominant triplen harmonic level in the subsequent parametric study.

Table 1. Classification of current harmonics and their impact on the neutral current in 3P + N networks.

Harmonic Group	Typical Orders	Behavior in Three-Phase System	Effect on Neutral Current
Fundamental	$h = 1$	120° phase shift between phases	Tends to cancel out under balanced load.
Non-triplen	$h \neq 3k$ (e.g., 5, 7, 11…)	$h \cdot 120^{\circ}$ phase shift	Partially cancels out in a symmetrical mode.
Triplen	$h = 3k$ (3, 9, 15…)	in-phase (zero-sequence)	Sums arithmetically in the neutral conductor (N), leading to a significant increase in I_N; under balanced conditions, $I_{N,3} \approx 3I_3$

2.2. Particularities of Triplen Harmonics

Triplen harmonics represent harmonic orders that are multiples of three, defined by the relationship:

$$h = 3k,\ k = 1, 2, 3, \ldots \quad (4)$$

These components frequently appear in low-voltage installations supplying single-phase non-linear loads (e.g., rectifiers with DC-link capacitors, switched-mode power supplies, LED drivers), as the current waveform is highly distorted, and lower-order harmonics (especially $h = 3$) can become dominant.

From the perspective of symmetrical components theory, triplen harmonics are associated with the zero-sequence. Unlike non-triplen harmonics, which are distributed in positive and negative sequences and tend to cancel out in a symmetrical three-phase system, triplen harmonics exhibit a specific behavior: they are in-phase across all three phases.

This result can be demonstrated starting from the phase shift in the h-th order harmonic between the phases of a three-phase system, which is h · 120°. For $h = 3k$, the following is obtained:

$$3k \cdot 120^{\circ} = k \cdot 360^{\circ} \quad (5)$$

which implies a phase rotation equivalent to an integer number of complete cycles.

Therefore, the triplen components on phases a, b, and c are co-phasal (they have the same phase angle). Consequently, at the neutral point (star connection), these components do not cancel each other out but tend to accumulate in the neutral conductor.

An important aspect is that this phenomenon can occur even when the loads are "balanced" in terms of the RMS values of the phase currents. RMS balance does not guarantee the cancelation of the neutral current in the presence of triplen harmonics, because the cancelation condition is phasor-based and depends on the distribution of harmonic components across the phases, not just on their total magnitudes [9]. Thus, in 3P + N networks within modern buildings, the neutral conductor can be significantly stressed due to 3rd-order harmonics and their multiples (9, 15, etc.).

This fact justifies their explicit analysis in the simulation methodology and in the interpretation of the results.

2.3. The Arithmetic Addition Mechanism in the Neutral Conductor

In a three-phase 3P + N network (star connection), the instantaneous current flowing through the neutral conductor is the algebraic sum of the instantaneous phase currents, according to Kirchhoff's Current Law applied at the neutral node:

$$i_N(t) = i_a(t) + i_b(t) + i_c(t) \quad (6)$$

where

- $i_N(t)$ represents the instantaneous value of the neutral conductor current;
- $i_a(t)$, $i_b(t)$ and $i_c(t)$ represent the instantaneous values of the currents in the three phases.

The above relationship highlights that the value of i_N(t) depends on both the magnitudes of the phase currents and the phase relationships among their components (fundamental and harmonics). Under a balanced linear mode, the fundamental components tend to cancel out, resulting in a negligible neutral current. Conversely, in the presence of unbalance or zero-sequence harmonics (particularly triplen harmonics), the sum can become non-zero and even significant, thereby justifying a distinct analysis between linear and non-linear operating modes.

For a useful formulation in the harmonic domain (RMS values), the following can be written for each harmonic order h:

$$I_{N,h} = |\ \vec{I}_{a,h} + \vec{I}_{b,h} + \vec{I}_{c,h}\ | \quad (7)$$

where $\vec{I}_{a,h}$, $\vec{I}_{b,h}$, $\vec{I}_{c,h}$ are the phasors of the h-th order harmonic currents on the three phases. This expression is particularly relevant for triplen harmonics ($h = 3k$), because, being in-phase across all three phases, they tend to add arithmetically in the neutral conductor [10].

For ideal linear 3P + N systems, the fundamental currents are phase-shifted by 120°. Under balanced conditions, these currents cancel out entirely at the neutral node, resulting in a negligible neutral current ($I_N \approx 0$). When the single-phase loads differ across the phases (unbalanced linear loads), a non-zero neutral current emerges; however, under a linear mode, this current remains strictly correlated with the degree of unbalance and typically does not exceed the maximum phase current. Understanding these baseline unbalanced conditions is essential before addressing complex harmonic compensation and source identification in modern power grids [11,12].

The Case of Non-Linear Loads: The Role of Triplen Harmonics

In the presence of non-linear loads, the phase current becomes non-sinusoidal and can be expressed (in a simplified form) as the sum of the fundamental component and harmonic components. Among these, the 3rd-order harmonic plays a dominant role in the overloading of the neutral conductor. To highlight this mechanism, let us consider separating the phase current into two main components:

$$i_a(t) = i_{a,1}(t) + i_{a,3}(t), i_b(t) = i_{b,1}(t) + i_{b,3}(t), i_c(t) = i_{c,1}(t) + i_{c,3}(t) \quad (8)$$

The instantaneous current flowing through the neutral conductor is:

$$i_N(t) = i_a(t) + i_b(t) + i_c(t) \quad (9)$$

Substituting the above relations yields:

$$i_N(t) = \underbrace{[i_{a,1}(t) + i_{b,1}(t) + i_{c,1}(t)]}_{(\approx 0 \text{ balanced mode})} + [i_{a,3}(t) + i_{b,3}(t) + i_{c,3}(t)] \quad (10)$$

For the fundamental component ($h = 1$), under balanced conditions, the currents are phase-shifted by 120° and their sum tends to zero. In contrast, for the 3rd-order harmonic (and, generally, for triplen harmonics $h = 3k$), the components across the three phases are in-phase (zero-sequence) [13]. Therefore, they do not cancel each other out in the vector sum, but rather add arithmetically in the neutral conductor, which leads to:

$$i_{N,3}(t) \approx i_{a,3}(t) + i_{b,3}(t) + i_{c,3}(t) \approx 3\, i_3(t) \quad (11)$$

$$I_{N,3} \approx 3I_3 \quad (12)$$

Consequently, the RMS current flowing through the neutral conductor can increase significantly and, under certain conditions, may exceed the phase current, even if the loads are apparently uniformly distributed across the phases in terms of RMS values.

The separation between the fundamental component (which cancels out in a balanced mode) and the triplen component (which adds arithmetically in the neutral conductor) is illustrated in Figure 1.

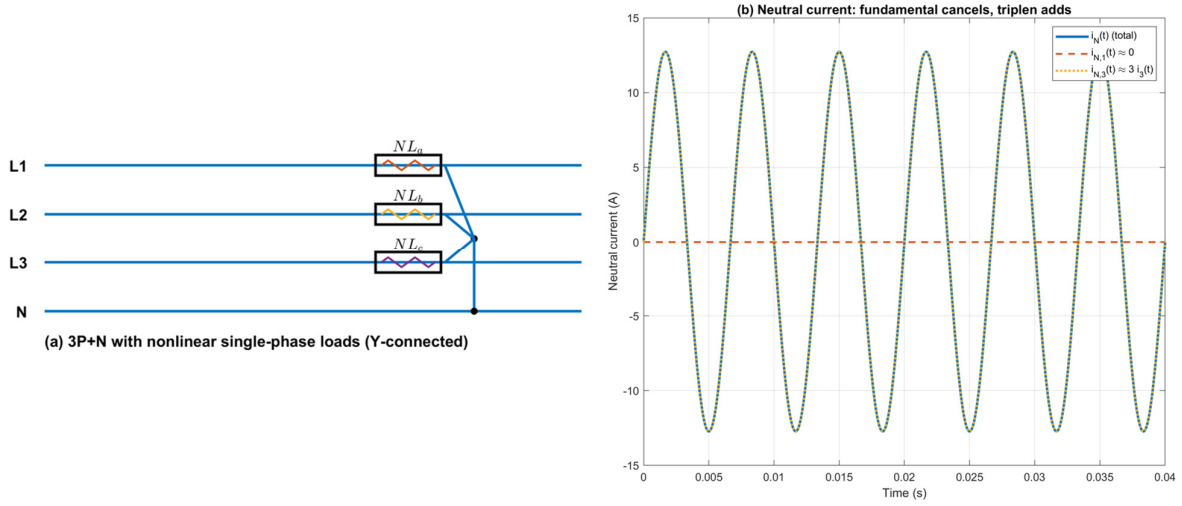

Figure 1. Nonlinear loads in a 3P + N system: while the balanced fundamental components cancel in the neutral conductor ($i_{N,1} \approx 0$), triplen harmonics ($h = 3k$) are in-phase and add arithmetically, resulting in a significant neutral current ($i_{N,3} \approx 3i_3$).

To quantify this phenomenon and to directly compare the severity of the neutral conductor overloading across different scenarios, this paper proposes the use of a specific index, termed the neutral loading factor (k_N) [14]. Its calculation method and its role as the primary evaluation metric within the BMS algorithm will be rigorously defined and detailed in the Methodology Section (Section 3.1.3).

Subsequently, this indicator will be correlated with H_3 (%) in the parametric study (scenario S3), leading to the graphical representation of k_N as a function of H_3 (%).

2.4. Implications for Power Losses and Conductor Heating

The increase in the neutral conductor current leads to a significant rise in Joule heating, as these power losses are directly proportional to the square of the RMS current. As a first

approximation, the copper losses for the neutral and phase conductors can be expressed as follows:

$$P_{Cu,N} = I_N^2 R_N, \qquad P_{Cu,ph} = \sum_{x \in \{a,b,c\}} I_x^2 R_x \tag{13}$$

where I_N is the RMS current flowing through the neutral conductor, I_x represents the RMS phase currents, and R_N, R_x denote the equivalent resistances of the neutral and phase conductors, respectively.

It is important to note that the current Simulink model evaluates the thermal impact strictly by quantifying the instantaneous Joule losses ($P = I^2 \cdot R$), expressed in Watts. These power losses serve as a direct and proportional indicator of the thermal stress applied to the insulation. The exact temperature variation in degrees Celsius is not dynamically simulated in this phase, as it depends on complex thermodynamic variables (e.g., ambient temperature, specific cable routing methods, and grouping factors) that fall beyond the purely electrical scope of this analysis [15,16].

Even if the phase conductors are correctly sized according to classical assumptions (predominantly sinusoidal loading and a lightly loaded neutral), a high I_N value can lead to:

- additional thermal losses within the cable and conduits;
- localized heating of accessories (terminals, clamps, neutral busbars), where contact resistances can amplify heat dissipation;
- accelerated insulation aging, particularly in congested cable routings and poorly ventilated spaces.

Crucially, the conductor's resistance increases with temperature, potentially creating a thermal feedback loop. Typically, the variation in resistance with temperature can be approximated by the following equation:

$$R(T) = R_{20}\left[1 + \alpha\left(T - 20\,^{\circ}\mathrm{C}\right)\right] \tag{14}$$

where:

- $R(T)$ is the resistance of the conductor at the operating temperature T;
- R_{20} is the nominal resistance of the conductor at the reference temperature of 20 °C;
- α is the temperature coefficient of resistance specific to the conductor material (e.g., for copper);
- T is the current temperature of the conductor, expressed in degrees Celsius (°C).

To establish a rigorous correlation between the electrical phenomena and their thermal impact, an evaluation based on Joule losses will be employed in the Results Section. This approach allows for highlighting the time evolution of the thermal stress applied to the neutral conductor under scenarios S2 and S3.

3. Materials and Methods

This section presents the methodology employed to investigate the influence of triplen harmonics on the current and thermal stress of the neutral conductor in low-voltage 3P + N networks [17].

The proposed approach combines an electrical model implemented in MATLAB/Simulink R2022a (MathWorks, Natick, MA, USA) with a testing framework based on controlled scenarios (S0–S3), ensuring that the contribution of the unbalance can be isolated from that of the triplen harmonics. To ensure the comparability of the results and the repeatability of the numerical experiments, the power supply and grid parameters are kept constant across all scenarios, varying only the load type and the imposed harmonic content. The indicators used in the evaluation include the current total harmonic distortion (*THD*i), the 3rd-order

harmonic content (H_3 (%)), the neutral current (I_N), and the neutral loading factor (k_N). The results are subsequently correlated with the dynamic evolution of Joule losses to assess the thermal stress on the neutral conductor.

3.1. Architecture of the Analyzed System and Modeling Assumptions

3.1.1. Description of the Analyzed Grid (3P + N, 50 Hz)

The investigated system is a three-phase low-voltage 3P + N network with a fundamental frequency f = 50 Hz, representative of indoor installations in modern buildings (residential or commercial), where power distribution to receivers is predominantly achieved through single-phase L–N circuits. Topologically, the network is modeled in a star connection with a common neutral conductor, such that the neutral current results from the sum of the phase currents, according to Equation (6) defined previously.

This configuration is highly relevant because, within "smart building" environments, the density of electronic loads (e.g., LEDs, IT equipment, switched-mode power supplies) is continuously increasing [18].

Consequently, the harmonic content of the phase currents can lead to significant stress on the neutral conductor, even under operating modes where the phase RMS currents are apparently balanced.

3.1.2. Modeling Assumptions and Their Justification

To isolate the phenomenon of interest (neutral overloading due to triplen harmonics) and to obtain reproducible results, the model adopts the following assumptions:

- Idealized power supply. The supply voltage is considered sinusoidal and symmetrical, with a 120° phase shift between phases. This choice allows the observed current distortions to be attributed primarily to the non-linear loads, thereby avoiding any ambiguity introduced by pre-existing voltage background distortions.
- Grid impedance representation. Although the model allows for the configuration of complex impedances (R-L), a purely resistive representation of the phase lines and the neutral conductor was chosen for the presented scenarios. Furthermore, for small conductor cross-sections (e.g., 1.5 mm^2) and the short routing lengths typical of indoor building installations, the inductive reactance (X_L) is physically negligible compared to the active resistance (R). This physical reality fully justifies the adoption of a purely resistive model. This approach facilitates the mathematical isolation of the neutral current summation phenomenon by eliminating the interference of additional inductive phase shifts, providing a clear framework for analyzing the flow of triplen harmonics.
- Building-specific L-N connections. Loads are connected as single-phase entities between each phase and the neutral, accurately reflecting the typical power consumption structure in modern buildings (multiple socket and lighting circuits, IT equipment, switched-mode power supplies, etc.). This assumption is essential because triplen harmonics are predominantly generated by single-phase non-linear loads and accumulate in the neutral conductor via the zero-sequence mechanism [19].
- Parametric control of the harmonic content. In scenarios S3 and S4, the loads are equivalently represented by imposed currents comprising a fundamental component and a 3rd-order harmonic component. This ensures that the H_3 proportion can be varied in a controlled and reproducible manner (as in S3), or maintained at severe levels during a simulated phase loss (as in S4). This approach does not aim to faithfully replicate the specific waveform of every equipment type, but rather to construct a numerical experimental framework where the influence of the 3rd harmonic on I_N and k_N can be quantified without underlying uncertainties.

The detailed configuration of the numerical model is illustrated in Figure 2. It highlights the interconnection among the power supply, the line impedances (simplified to a resistive level), and the data acquisition system. The use of controlled current sources to impose the desired harmonic profile on each phase can be observed, thus enabling the precise monitoring of the resulting current in the neutral conductor via the dedicated out.iN sensor [20].

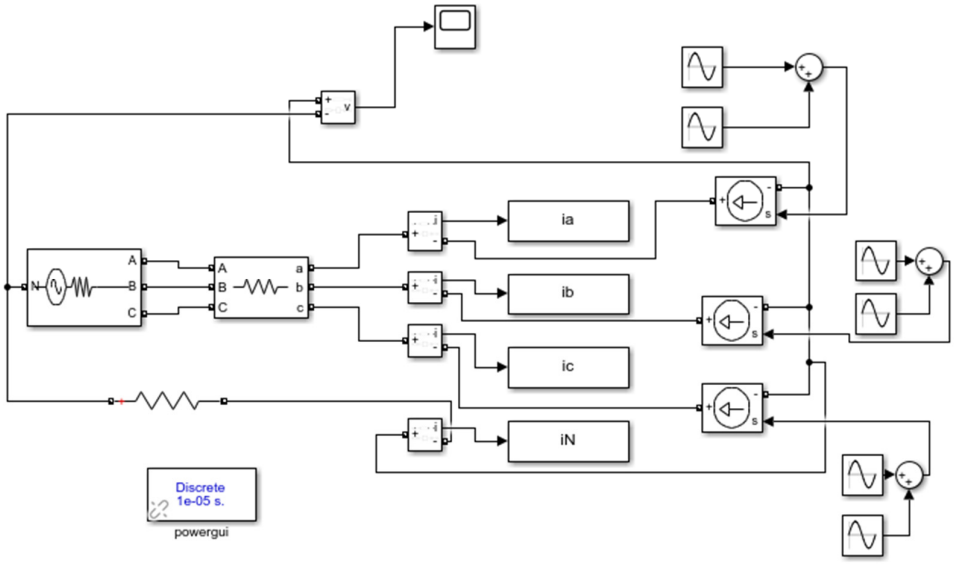

Figure 2. Block diagram of the simulation model implemented in MATLAB/Simulink for harmonic analysis in 3P + N networks, including the three-phase power supply, purely resistive line impedances, measurement sensors, and controlled non-linear loads.

3.1.3. Monitored Variables and Evaluation Criteria

In all scenarios, the instantaneous phase and neutral currents are monitored: $i_a(t)$, $i_b(t)$, $i_c(t)$, $i_N(t)$. From these, RMS values I_a, I_b, I_c, I_N, the harmonic indicators (THD_i, H_3 (%)) and the neutral loading factor are determined:

$$k_N = \frac{I_N}{I_{ph}} \tag{15}$$

where:

- k_N (Neutral loading factor): It is a dimensionless indicator that quantifies the stress on the neutral conductor relative to a reference phase current value. This allows for the rapid identification of operating modes where the neutral becomes more thermally stressed than the system's phases ($k_N > 1$).
- I_N (Neutral conductor current): Represents the RMS value of the current flowing through the installation's neutral point. In the presence of non-linear loads, this quantity is determined by the arithmetic addition of the triplen harmonics (orders 3, 9, 15, etc.), which are in-phase across all three phases (zero-sequence).
- I_{ph} (Reference phase current): Represents a unitary reference value for the phase current, defined identically across all simulation scenarios. The use of a constant value for I_{ph} throughout the tests ensures the comparability of the results and allows for the direct observation of how the increase in harmonic distortion affects the cable's thermal balance [21].

In the Results Section, these variables are analyzed in correlation with the Joule losses in the neutral conductor and the resulting power dissipation in the relevant scenarios (S2, S3 and S4).

3.2. Electrical Model in MATLAB/Simulink

The numerical implementation of the proposed architecture was carried out in the MATLAB/Simulink R2022a environment, using the Simscape Electrical (Specialized Power Systems) library. The model is configured for a time-domain simulation, utilizing a Discrete-type solver managed by the powergui block.

The choice of the discrete mode, with a sampling step of 1×10^{-5} s, ensures sufficient temporal resolution to accurately capture the oscillations of the 3rd-order harmonic (150 Hz).

3.2.1. Model Components and Their Functional Role

- Voltage source (Three-Phase Voltage Source): Models the power supply network as an ideal voltage source in a star connection, with a grounded neutral, ensuring the symmetry and balance of the phase voltages.
- Line and neutral impedances: The electrical routings are represented by Three-Phase Series RLC Branch blocks and a single-phase RLC block for the neutral. In the current configuration, these are set as pure resistances (R), eliminating numerical instabilities that may arise when injecting harmonic currents into inductive branches and providing a clear perspective on the algebraic summation of currents at the neutral point.
- Data acquisition system: The use of Current Measurement blocks connected in series on each phase and the neutral allows for the extraction of instantaneous signals to the Workspace as timeseries objects (out.ia, out.ib, out.ic, out.iN).
- Controlled non-linear loads: Each phase is loaded via a Controlled Current Source.

The control signal is generated by summing two sinusoidal functions:

- A fundamental component at 50 Hz (representing the nominal active load).
- A 3rd-order harmonic component at 150 Hz (representing the harmonic distortion introduced by electronic equipment).

The parameters used to validate the model in the baseline scenario are summarized in Table 2.

Table 2. Nominal parameters of the simulation system.

Parameter	Symbol	Value/Unit
Nominal phase voltage (RMS)	U_{ph}	230 [V]
Fundamental frequency	f_1	50 [Hz]
Equivalent phase resistance	R_{ph}	0.1 [Ω]
Neutral conductor resistance	R_N	0.1 [Ω]
Fundamental current amplitude	I_{max_1}	13 [A]
3rd-order harmonic amplitude	I_{max_3}	13 [A]
Discrete simulation step	T_s	10^{-5} [s]

3.2.2. Decision Algorithm and BMS Integration

To prevent the thermal risks associated with triplen harmonics, this paper proposes a proactive decision algorithm designed for integration into Building Management Systems (BMS) [22,23]. The algorithm utilizes the k_N indicator (the ratio of neutral current to phase current), calculated in real-time, to evaluate the stress level of the neutral conductor and to initiate preventive actions before the triggering of conventional protections or the degradation of insulation. The flowchart of this algorithm is illustrated in Figure 3.

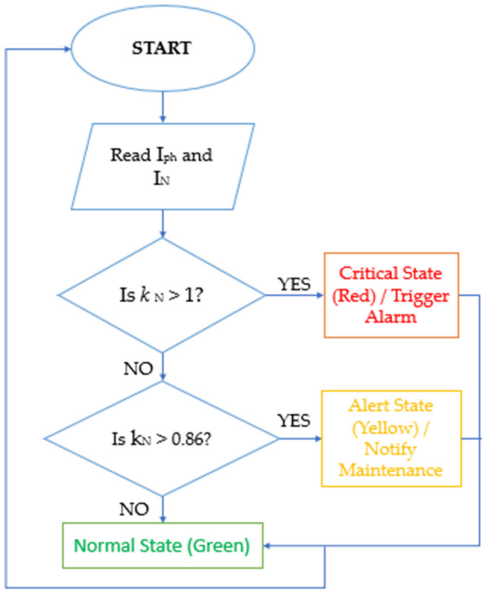

Figure 3. Flowchart of the BMS decision algorithm based on the monitoring of the k_N parameter.

From an operational perspective, the automation algorithm classifies the installation's status into three distinct operating zones, based on the instantaneous value of k_N and its correlation with the 3rd-order harmonic content (H_3):

- Green Zone (Normal Operation/Passive Monitoring): Defined for $k_N < 0.86$ (corresponding to a 3rd-order harmonic level $H_3 < 30\%$). In this mode, the current flowing through the neutral conductor is well below the cable's thermal limit. The BMS only logs the data for the consumption history, without requiring active interventions.
- Yellow Zone (Alert State/Preventive Action): Defined for $0.86 \leq k_N < 1.0$ (typically corresponding to an H_3 between 30% and 33%). The neutral current dangerously approaches the maximum allowable ampacity (I_z). The BMS triggers maintenance alarms for the technical staff and may activate filtering solutions (if active harmonic filters are present in the installation) to mitigate the distortion before the critical threshold is reached [24].
- Red Zone (Critical State/Active Intervention—Load Shedding): Defined for $k_N \geq 1.0$ (a scenario where the neutral current exceeds the phase current, as explicitly demonstrated by the extreme conditions in Scenario S4). This represents an imminent risk of overheating and fire. In this phase, the BMS automatically transitions from monitoring to active protection, initiating load shedding procedures (the automatic sequential disconnection of non-essential non-linear loads) to force the neutral current back below the safety limit.

This decision matrix prevents the nuisance tripping of main circuit breakers and ensures power supply continuity for critical consumers, directly addressing the root cause of the overload before the thermal effect becomes irreversible.

3.3. Controlled Generation of the 3rd-Order Harmonic via Controlled Current Sources

To conduct the parametric study and the extreme stress test (scenarios S3 and S4), a method is required that allows for the deterministic and reproducible variation in the harmonic content, specifically the 3rd-order harmonic, without relying on the internal parameters of a non-linear model (e.g., DC bus capacitor values, DC load, parasitic impedances, etc.). To this end, the loads are equivalently represented by controlled current sources connected as single-phase entities between each phase and the neutral conductor, and the phase current is explicitly imposed as the sum of the fundamental component and

the 3rd-order harmonic component [25,26]. Although modeled via controlled current sources to ensure precise parametric variation, this configuration acts as the mathematical and electrical equivalent of a typical single-phase bridge rectifier with a capacitive filter (Figure 4)—the standard topology for modern Switch-Mode Power Supplies (SMPS) and IT equipment. This simplified schematic, utilizing an ideal voltage source, is presented specifically to isolate and demonstrate the pure harmonic current generation mechanism of the load, independent of the grid's internal impedances. To characterize the severity of the non-linear load under extreme conditions (Scenario S4), the Crest Factor (CF) was evaluated. The simulated load exhibits a high CF of 1.89, derived from the ratio between the instantaneous peak current (~42.4 A) and the resulting RMS value (22.36 A). This value accurately reflects the highly impulsive, pulsating nature of modern non-linear loads compared to the standard 1.41 CF of a pure sine wave.

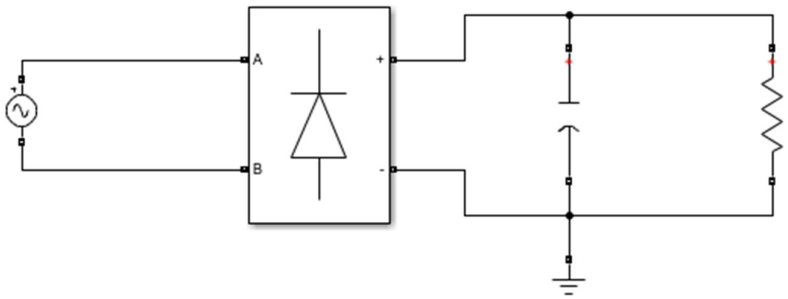

Figure 4. Equivalent electrical diagram of the non-linear load structure (single-phase bridge rectifier with capacitive filter) represented mathematically in the simulation.

This approach enables direct control over the H_3 (%) indicator and allows for the establishment of a clear quantitative relationship among H_3 (%), the neutral current I_N, and the neutral loading factor k_N.

Equations of the Imposed Currents (RMS)

The imposed current on each phase is defined by the summation of the fundamental component ($f_1 = 50\,\text{Hz}$) and the 3rd-order harmonic component ($3f_1 = 150\,\text{Hz}$). Using the RMS values I_1 and I_3, the instantaneous currents across the three phases are:

$$\begin{aligned} i_a(t) &= \sqrt{2}\, I_1 \sin(\omega t) + \sqrt{2}\, I_3 \sin(3\omega t) \\ i_b(t) &= \sqrt{2}\, I_1 \sin\left(\omega t - \tfrac{2\pi}{3}\right) + \sqrt{2}\, I_3 \sin(3\omega t - 2\pi) \\ i_c(t) &= \sqrt{2}\, I_1 \sin\left(\omega t + \tfrac{2\pi}{3}\right) + \sqrt{2}\, I_3 \sin(3\omega t + 2\pi) \end{aligned} \tag{16}$$

where $\omega = 2\pi f_1$. Because $\sin(3\omega t \pm 2\pi) = \sin(3\omega t)$, it follows that the 3rd-order harmonic is perfectly in-phase across all three phases (zero-sequence component), which justifies its inclusion as the central element in analyzing the stress on the neutral conductor.

The proportion of the 3rd-order harmonic is quantified by the H_3 (%) indicator (previously defined by Equation (3) in Section 2.1).

In the parametric scenario S3, the H_3 (%) value is systematically varied within a predetermined range, while keeping the fundamental component I_1 constant, in order to explicitly highlight the effect of the triplen harmonic on the neutral current [27].

Although the general definition of total harmonic distortion (*THD*i) encompasses the sum of all higher harmonic orders, a simplified form of this indicator is employed within the analyzed non-linear scenarios (S3 and S4). Given that the model exclusively injects

the 3rd-order harmonic to isolate its effect, the *THD*i becomes a direct ratio between this component and the fundamental one:

$$THD_i = \frac{I_{3,RMS}}{I_{1,RMS}} \cdot 100\% \quad (17)$$

where:

- THD_i is the Total Harmonic Distortion of the current, expressed as a percentage;
- I_3 is the RMS value of the 3rd harmonic component (corresponding to 150 Hz);
- I_1 is the RMS value of the fundamental phase current (corresponding to 50 Hz).

Note: This simplification is justified because the simulated phase currents contain no other disturbing components besides the 3rd-order harmonic.

The synthesis process of the non-linear load, mathematically defined by Equation (16), guarantees the spectral purity of the injected signal. This approach ensures that the summation phenomenon within the neutral conductor is isolated and analyzed without interference from other higher-order harmonic components.

As theoretically demonstrated in Section The Case of Non-Linear Loads: The Role of Triplen Harmonics, applying Kirchhoff's laws at the neutral node results in the cancelation of the balanced fundamental component and the arithmetic summation of the zero-sequence harmonics ($I_{N,3} \approx 3I_3$). Both the parametric study (S3) and the extreme stress test (S4) within the Simulink model is constructed upon this physical principle. By systematically varying the parameters of the current sources, the objective is to extract the direct quantitative correlation among the 3rd-order harmonic proportion (H_3 (%)), the resulting current measured on the neutral conductor (I_N), and the neutral loading factor (k_N) [28,29].

3.4. Measurement Configuration and Harmonic Analysis

To obtain accurate results, the data acquisition and processing procedure within the simulation environment was configured to comply with the requirements of spectral analysis and RMS value calculation.

3.4.1. Determination of Root-Mean-Square (RMS) Values

The measurement of the RMS values for the phase currents (I_a, I_b, I_c) and the neutral current (I_N) was performed by processing the instantaneous signals extracted to the MATLAB Workspace as timeseries objects.

The calculation of the RMS value was carried out based on the standard definition, utilizing a sliding window equal to the fundamental period (T = 0.02 s):

$$I_{RMS} = \sqrt{\frac{1}{T}\int_{t-T}^{t} i^2(\tau)d\tau} \quad (18)$$

where:

- I_{RMS} represents the calculated RMS current value;
- T is the fundamental period of the signal (T = 0.02 s for the 50 Hz grid frequency);
- t is the current simulation time;
- i_τ represents the instantaneous value of the current at the integration time τ.

This method ensures the extraction of stable indicators, which subsequently serve as input data for the previously presented sizing tables (Table 3).

Table 3. Ampacity (I_z) for copper conductors (90 °C insulation) according to the degree of harmonic pollution.

Cross-Section [mm^2]	I_z for THD$_i$ < 15% [A]	I_z for 15% < THDi < 33% [A]	*Iz* for THD$_i$ > 45% [A]
1.5	23	19.8	13
2.5	32	27.5	18
4	42	36.1	24

The sizing process for conductors in the presence of 3rd-order harmonics follows the logic of derating the ampacity, as the neutral current induces additional thermal losses that are not present under purely sinusoidal conditions. In this paper, a 1.5 mm^2 cable (XLPE insulation, installed in free air) is used as a reference, for which the baseline ampacity (I_z) is 23 A in the absence of harmonics [30,31].

The impact of triplen harmonics on this conductor is quantified by the following rules extracted from the analyzed technical standards:

- Case 1 ($THD_i \leq 15\%$): The harmonics have a negligible impact. The sizing current remains equal to the phase current, and the safety limit is the nominal 23 A.
- Case 2 ($15\% < THD_i \leq 33\%$): A derating factor of 0.86 is applied. The actual ampacity of the cable decreases to approximately 19.8 A (23 A × 0.86). Although the phase current might be below this value, the summation of harmonics on the neutral begins to thermally stress the cable significantly.
- Case 3 ($THD_i > 45\%$): This is the critical scenario simulated in the present study (S3). Under this operating mode, the neutral current becomes the primary sizing parameter, and the allowable ampacity of the conductor drops drastically to 13 A. This situation significantly exceeds the equality point $k_N = 1$, representing an extremely dangerous operating mode for insulation integrity.

This approach is essential to demonstrate that, although the measured phase currents may appear safe, the neutral current resulting from triplen harmonics can reach the critical threshold of 13 A, pushing the conductor to the limit of its thermal stability [32].

Furthermore, as will be demonstrated in the extreme test case (Scenario S4), the simultaneous occurrence of phase loss and severe harmonic pollution can force the neutral current up to 22.36 A, catastrophically exceeding this 13 A derated safety limit.

3.4.2. Spectral Analysis via the FFT Algorithm

The harmonic analysis was conducted using the FFT Analysis tool integrated within the powergui block. The analysis configuration incorporated the following critical settings:

- Fundamental frequency: Set to 50 Hz.
- Analysis window: A time interval starting after the moment t = 0.04 s was selected to ensure the elimination of initial transient modes and to analyze the system under steady-state conditions.
- Number of cycles: The spectral analysis was performed over 2 complete cycles of the fundamental frequency, providing optimal spectral resolution for the identification of the 3rd-order harmonic (150 Hz).

Through this procedure, the key indicators were determined: the *THD*i (Total Harmonic Distortion) and the individual proportion of the 3rd-order harmonic (H_3 (%)), which form the basis of the parametric study S3 and the extreme stress test (S4).

Due to the discrete simulation step set to 1×10^{-5} s, the model avoids the aliasing effect and ensures a high-fidelity representation of the neutral signal, even at triple the fundamental frequency [33,34]. Synchronizing the FFT analysis window with the zero-

crossings of the signal guarantees the phasor accuracy of the results presented in the subsequent section.

3.5. Definition of the Simulation Scenarios (S0–S4)

To rigorously evaluate the summation phenomenon of triplen harmonics within the neutral conductor, the testing methodology was structured in a logical progression, advancing from ideal conditions to critical operating modes. This stratification of the simulations enables the isolation of variables and the precise identification of the point at which harmonic pollution becomes the determining factor in the thermal stress applied to the installation [35].

3.5.1. Testing Scenarios Matrix

Each scenario was designed to address a specific question regarding the loading degree of the neutral conductor. The parametric details and technical objectives are summarized in Table 4.

Table 4. Simulation scenarios matrix and analysis objectives.

Scenario	Designation	Parametric Configuration (I_1, I_3)	Technical Objective and Validation
S0	Baseline mode	I_1 = 10 A (balanced), I_3 = 0 A	Validation of the model's perfect balance; the neutral current must be zero ($I_N \approx 0$).
S1	Linear unbalance	I_1 unbalanced (e.g., 12, 10, 8 A), I_3 = 0 A	Quantification of the neutral current caused exclusively by phase asymmetry in the absence of harmonics.
S2	Moderate harmonic mode	I_1 = 10 A, I_3 = 3 A (THDi ≈ 30%)	Analysis of the mode where the 0.86 derating factor is applied according to standards.
S3	Critical harmonic mode	I_1 = 10 A, I_3 varied up to 10 A	Identification of the threshold where I_N reaches the 13 A limit for the 1.5 mm^2 conductor.
S4	Extreme unbalance and severe harmonics	Phases 1 and 2: I_{fund} = 10 A, I3rd = 10 A Phase 3: Disconnected (I = 0 A)	Evaluation of massive neutral current accumulation during simultaneous severe unbalance (phase loss) and non-linear loading, demonstrating the necessity of dynamic BMS intervention.

3.5.2. Rationale for the Parametric Scenario S3

Scenario S3 represents the core element of the study, designed as a stress test for the electrical infrastructure. Within this scenario, the proportion of the 3rd-order harmonic is increased in a controlled manner to simulate the intensive use of IT equipment and LED lighting systems.

The importance of this scenario lies in verifying the hypothesis that, in the presence of triplen harmonics, the neutral current can exceed the phase current, thereby invalidating classical sizing models. By varying I_3, the model aims to demonstrate the point at which the RMS value of the neutral current exceeds 13 A. This value is considered critical because it represents the maximum safe operating limit for a 1.5 mm^2 conductor under severe harmonic pollution conditions (H_3 > 45%), a threshold beyond which the insulation integrity is compromised [36,37]. Building upon the logic of S3, Scenario S4 is introduced as the ultimate stress test. While S3 explores the gradual increase in harmonics, S4 simulates

a catastrophic operational state (phase loss combined with peak harmonic distortion) to validate the BMS responsiveness under conditions that far exceed the theoretical safety thresholds discussed in the following sections.

3.5.3. Performance Indicators Monitoring

For each scenario, the model automatically extracts the following indicators, which substantiate the active management logic across all testing conditions, including the extreme stress test (S4):

- Neutral loading factor (k_N): The ratio between the neutral current and the phase current, utilized as a control variable for automation.
- Harmonic distortion (H_3 (%)): The proportion of the 3rd-order harmonic relative to the 50 Hz fundamental.
- Joule losses in the neutral ($P_{Cu,N}$): A parameter used to evaluate the energy efficiency of Smart Buildings.

3.6. Establishing Thermal Safety Limits (Benchmark)

The performance and safety of the proposed model are evaluated in relation to the actual thermal capacity of the reference conductor used in the simulation (1.5 mm^2 cross-section). Table 5 summarizes the current thresholds identified as critical for maintaining the installation's integrity, translating the physical limits of the cable into configuration parameters for the smart protection system [38–40].

Table 5. Current thresholds and safety limits for the management of distribution risers.

System State	Current Value (I_N) [A]	Technical Significance and Operational Impact
Nominal ampacity	23	Reference for pure sinusoidal conditions, without harmonic distortions.
Derated ampacity	19.8	Maximum allowable limit under moderate harmonic pollution conditions ($H_3 \approx 30\%$).
Critical regulatory limit	13	Safety threshold for severe harmonic conditions ($H_3 > 45\%$), beyond which the risk of fire is imminent.

The implementation of these benchmarks facilitates the transition from the static sizing of electrical installations to the dynamic management of Smart Building infrastructure. Consequently, the continuous monitoring of the harmonic content becomes the foundation for automatically adjusting the operating limits, defining the "Safe-by-Design" concept explored in this research. The robustness of these benchmarks is specifically challenged in Scenario S4, where the combined effect of phase loss and triplen harmonics is used to verify if the BMS correctly identifies the transition from the 'Derated ampacity' zone directly into the 'Critical regulatory limit' and subsequent alarm state.

4. Results and Simulation Validation

This section centralizes and analyzes the results obtained from executing the numerical model. Although the research encompassed the evaluation of four distinct scenarios (S0–S4), ranging from the ideal sinusoidal mode to critical pollution levels, the present analysis focuses primarily on scenarios S2 and S3.

This selection is justified because scenarios S0 (ideal mode, no harmonics) and S1 (minimal pollution, within regulatory limits) serve as fundamental baselines, confirming the model's stability under safe operating conditions. In contrast, scenarios S2 and S3 represent

the critical decision-making situations for a Smart Building, explicitly highlighting the alarm and intervention thresholds of the automation system [41,42].

4.1. Waveform Analysis and the Summation Phenomenon (Scenario S2)

The initial stage of validation consists of analyzing the system's behavior under the influence of moderate harmonic pollution, corresponding to scenario S2 (where $THDi \approx 30\%$). This operating mode is representative of the nominal conditions in a modern office building, where the load profile is predominantly non-linear (e.g., LED lighting, IT equipment, and switched-mode power supplies) [43,44].

The simultaneous evolution of the instantaneous phase currents and the resulting current flowing through the neutral conductor under Scenario S2 are comprehensively illustrated in the subsequent figures (detailed in the updated Figure 5).

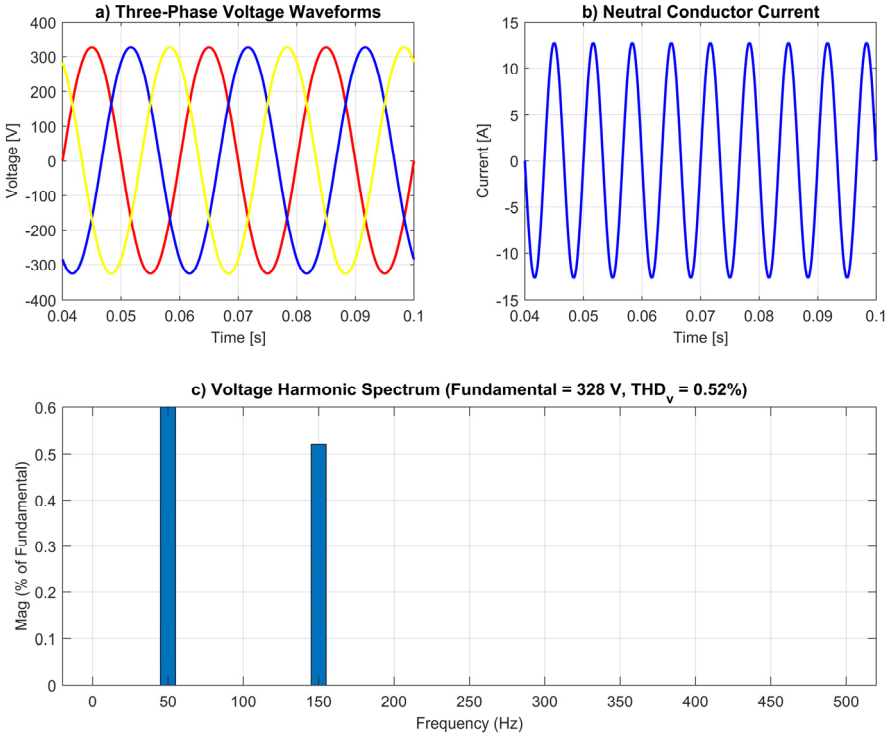

Figure 5. Simulated waveforms and harmonic analysis at the load terminals under Scenario S2: (**a**) Three-phase voltage waveforms; (**b**) Neutral conductor current; (**c**) Corresponding voltage harmonic spectrum ($THD_V = 0.52\%$). Note: The red, blue, and yellow lines represent phases A, B, and C, respectively.

The analysis of the waveforms obtained from the simulation of scenario S2 (moderate harmonic mode) highlights three fundamental technical aspects that validate the integrity of the numerical model. First, a pronounced deformation of the phase waveforms is observed, where the non-sinusoidal nature of the line currents is marked by narrow and "sharp" peaks. This phenomenon is characteristic of non-linear loads that draw energy only in the proximity of the peak voltage value, confirming the accurate modeling of rectifiers with capacitive filtering [45,46].

A critical observation concerns the frequency of the neutral current (i_N); although the phase currents operate at the fundamental frequency of 50 Hz, the neutral current exhibits a dominant frequency of 150 Hz, providing visual evidence of the presence of 3rd-order harmonics (triplen harmonics).

Finally, the results demonstrate the harmonic summation phenomenon: although the system is balanced, with phase RMS values of approximately 10 A, the neutral current

does not cancel out, but rather reaches an RMS value of 8.6 A. This accumulation is caused by the fact that the 3rd-order harmonics are in-phase (zero-sequence), leading to their arithmetic summation at the neutral point. Furthermore, obtaining a ratio of k_N = 0.86 (8.6 A/10.0 A) validates the system's entry exactly at the threshold of the Yellow Zone (Alert State), confirming the necessity of the proactive intervention by the previously described BMS algorithm.

Furthermore, while the primary focus of this study is the thermal stress on the neutral conductor caused by current harmonics, it is imperative to acknowledge their secondary effect on the system's overall voltage quality. As the highly distorted current flows through the installation's equivalent impedance, it generates non-sinusoidal voltage drops. Figure 5 illustrates the voltage waveform at the load terminals under the S2 scenario. As observed, the voltage waveform remains predominantly sinusoidal, with a Total Harmonic Distortion (*THD*v) of approximately 0.52%. This indicates that, although the load current is highly distorted in this scenario, the voltage quality is not yet significantly affected, remaining well within the standard limits for power quality.

In parallel with the phase voltage degradation, the massive accumulation of harmonic currents induces a significant voltage drop along the neutral conductor itself. Figure 6 presents the simulated neutral-to-ground voltage waveform (V_N). While in an ideal, balanced linear system this voltage would remain near zero, our simulation results validate that triplen harmonics generate a highly distorted, non-zero neutral voltage. This condition poses severe power quality issues for sensitive IT equipment and introduces potential safety hazards.

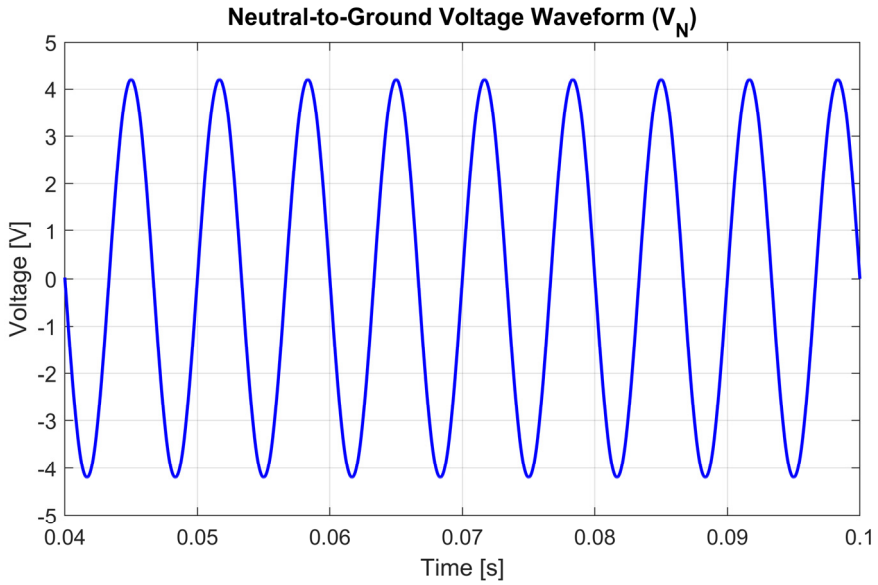

Figure 6. Neutral-to-ground voltage waveform (V_N) generated by the triplen harmonic currents flowing through the neutral conductor's impedance.

To provide a comprehensive overview of the impact of non-linear loads on the overall three-phase system, Figure 7 presents the voltage and current waveforms for all three phases, as monitored at the load terminals. This simultaneous representation enables the observation of the distortion symmetry and the pulsating nature of the phase currents—elements that confirm the severity of the distorting mode analyzed under Scenario S2 and provide a foundation for the detailed spectral analyses presented in the subsequent section.

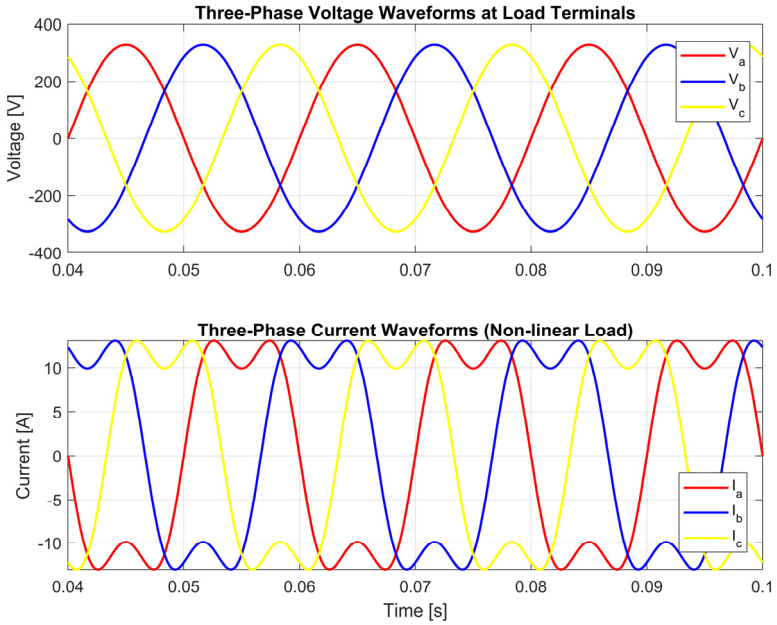

Figure 7. Three-phase voltage (**top**) and current (**bottom**) waveforms at the load terminals, illustrating the combined impact of non-linear loads on the system behavior.

4.2. Spectral Characterization of Harmonic Pollution (S2)

To quantify the distribution of the harmonic components observed in the previously presented waveforms, an analysis using the Fast Fourier Transform (FFT) was performed. This step enables the precise identification of the harmonic orders that contribute to the increase in the neutral current, as well as the calculation of the total harmonic distortion index (*THD*i).

The analysis was conducted using the FFT Analysis tool within the powergui block, focusing on the spectrum of both the phase current and the neutral current for scenario S2. The results are summarized in the Figures 8 and 9 below.

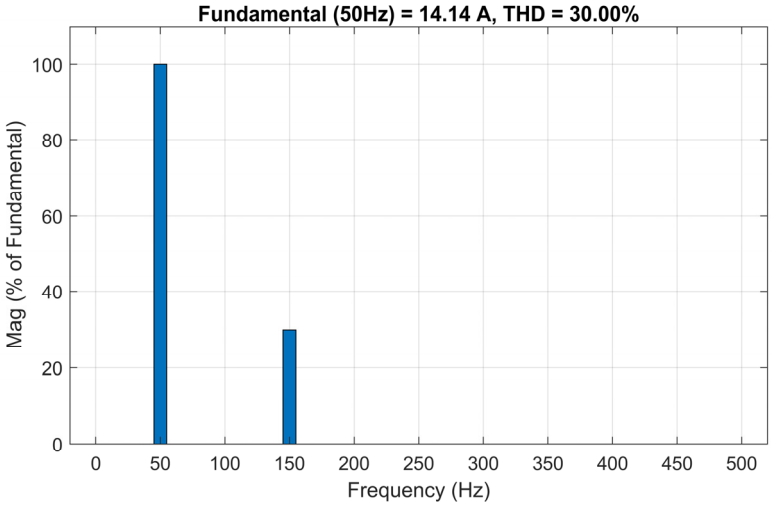

Figure 8. Frequency spectrum of the phase current for scenario S2 (Fundamental at 50 Hz).

The spectral analysis of the phase current (Figure 8) quantitatively confirms the non-sinusoidal nature of the current. The value of the fundamental component at 50 Hz is 14.14 A (the peak amplitude corresponding to the nominal RMS current of 10 A), while the total harmonic distortion (*THD*) index reaches the 30.00% threshold. It is observed that the distortion is caused almost exclusively by the 3rd-order harmonic (150 Hz), with the

remaining components (such as the 5th and 7th orders) having a negligible share in this operating mode [47].

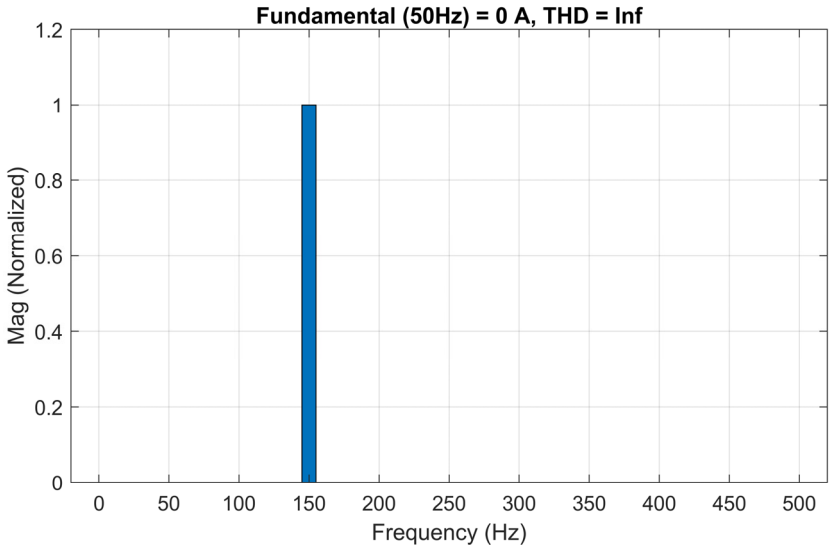

Figure 9. Frequency spectrum of the neutral current for scenario S2 (Dominance of the 150 Hz harmonic).

For a comprehensive validation of the summation phenomenon, the spectral composition of the current flowing through the neutral conductor (i_N) was additionally analyzed.

Comparing the two spectra reveals a clear distinction between the nature of the two currents. While the 50 Hz component is dominant on the phase, the fundamental is practically zero in the spectrum of the neutral conductor (Figure 9) due to load balancing. The fact that the *THD* indicator theoretically tends towards infinity (displayed as *THD* = Inf by the simulation environment) is the mathematical consequence of referencing the harmonic content (150 Hz) to a fundamental component (50 Hz) of zero value. The absolute dominance of the 150 Hz frequency within the neutral demonstrates that this current is the direct result of the arithmetic summation of the three zero-sequence harmonics originating from the phases.

This spectral characterization is essential for the Smart Building management system. The distortion value of 30% (predominantly $H_3 \approx 30\%$) generates a loading factor of $k_N = 0.86$, which serves as a precise reference threshold for activating the Alert State (Yellow Zone). Consequently, the BMS algorithm is notified that, although the thermal limits of the phases are not exceeded (10 A RMS), the neutral current already reaches 8.6 A, signaling an overloading trend that requires active monitoring [48].

4.3. Parametric Study: Evolution of the k_N Indicator as a Function of the H_3 Harmonic Proportion

To provide a mathematical foundation for the alarm thresholds implemented in the monitoring system, a parametric study on the evolution of the k_N ratio was conducted. This indicator is defined as the ratio between the RMS value of the neutral current and that of the phase current ($k_N = I_N/I_{ph}$) and represents the most relevant factor in assessing the risk of neutral conductor overload (Figure 10).

The analysis of the graph confirms the boundaries of the operating zones managed by the BMS algorithm, as previously defined in Section 3. As observed, the curve intersects the Alert Threshold ($k_N = 0.86$) at a harmonic content of $H_3 \approx 30\%$, marking the system's transition from the Green Zone to the Yellow Zone. Subsequently, the Mathematical Equality Point ($k_N = 1.0$), which triggers the critical state (Red Zone), is reached at $H_3 \approx 35.3\%$. Beyond this threshold, the neutral becomes consistently overloaded compared to the phases.

Within this red zone, upon reaching the extreme regulatory limit (H_3 = 45%), the value k_N = 1.23 indicates a 23% overload of the neutral relative to the phase, fully justifying the necessity of the severe cable derating measures imposed by standards [49].

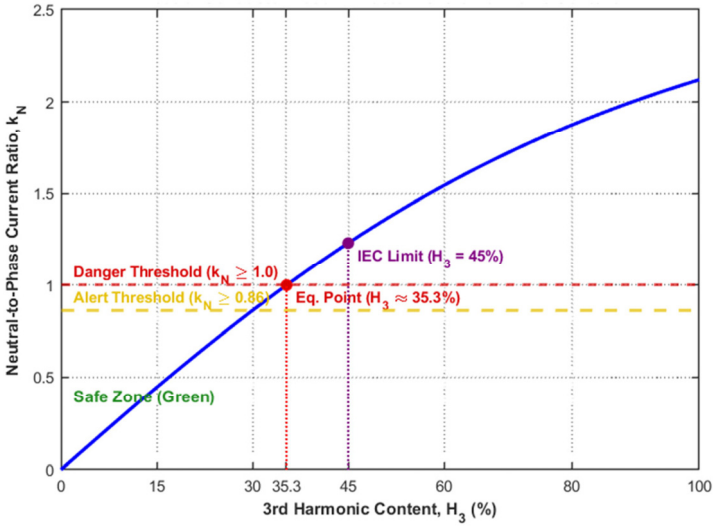

Figure 10. Evolution of the k_N ratio as a function of the 3rd-order harmonic proportion (H_3).

The results of this parametric study highlight the inadequacy of exclusively monitoring the phase current in the context of modern buildings, where non-linear loads predominate. The k_N indicator thus emerges as a fundamental control parameter within the proposed automation algorithm, facilitating the proactive protection of the installation. By utilizing this ratio, the system can identify and mitigate the thermal risks applied to the neutral conductor before they reach destructive thresholds.

4.4. Thermal Impact Analysis and Implications for Operational Safety

The transition from the purely electrical analysis of currents to the evaluation of the thermal impact is essential to understand the risks associated with harmonic pollution in modern buildings. The evolution of Joule losses was calculated to quantify the thermal stress exerted on the conductors, particularly in high distortion scenarios. The dynamics of these losses in relation to the control thresholds implemented in the BMS model are presented in Figure 11.

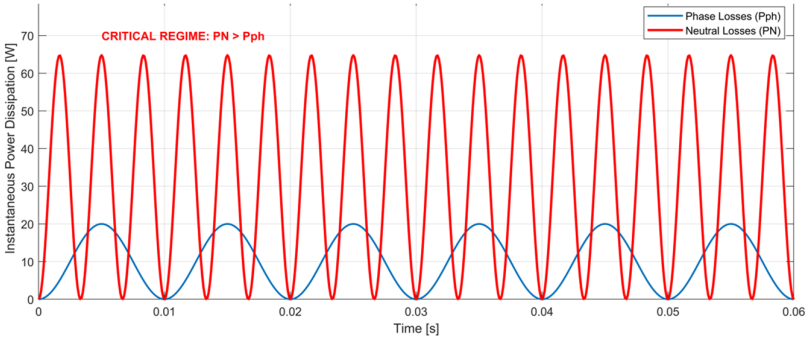

Figure 11. Comparative analysis of Joule losses in the phase conductor (P_{ph}) versus the neutral conductor (P_N) for Scenario S3.

The analysis of the obtained results highlights a major thermal vulnerability within standard electrical infrastructure, particularly regarding 1.5 mm^2 cross-section conductors, which are conventionally sized exclusively for phase currents under sinusoidal conditions.

In the presence of severe 3rd-order harmonic distortion (triplen harmonics), the neutral conductor—despite sharing the same cross-section as the phases—experiences a current density that exceeds its nominal thermal dissipation capacity under steady-state conditions. This phenomenon is visually documented in Figure 11 for the extreme scenario (S3). It can be observed that the instantaneous power losses in the neutral conductor reach peak values of approximately 65 W, being more than three times higher compared to the losses in the phase conductor (maximum 20 W). This massive thermal overload, invisible to conventional protection systems, induces a progressive increase in the operating temperature, thereby accelerating the thermal degradation process of the PVC polymeric insulation [50,51].

From an operational safety perspective, these operating conditions generate a latent risk of insulation failure, inevitably leading to short-circuits or fire incidents within cable routing systems (e.g., cable trunking, protective conduits). These data provide the necessary technical justification for implementing an active management strategy via the BMS. Unlike conventional thermomagnetic protection devices, which exhibit critical latency or even an inability to detect overcurrents on the neutral conductor, the proposed algorithm, based on the k_N indicator, functions as a proactive protection layer. By initiating automatic mitigation measures, such as disconnecting non-essential loads or activating active filters upon reaching the "Red Zone", the system ensures the infrastructure's integrity during a timeframe in which classical protections remain inactive. Consequently, the presented methodology transforms the building management system from a mere monitoring tool into a fundamental component of the electrical safety architecture.

4.5. Extreme Asymmetry and Harmonic Pollution (Scenario S4)

To further validate the BMS algorithm under the most severe operational conditions, a new test scenario (S4) was introduced, simulating the simultaneous presence of extreme unbalance and severe non-sinusoidal currents. In this scenario, Phase 3 is completely disconnected ($I_3 = 0$), while Phase 1 and Phase 2 supply highly distorted non-linear loads (10 A fundamental and 10 A 3rd harmonic).

The simulation results (Figure 12) reveal a critical accumulation phenomenon. While the RMS current on the two active phases is 14.14 A, the arithmetic summation of the zero-sequence harmonics, combined with the fundamental unbalance, forces the neutral current (I_N) to an extreme RMS value of 22.36 A (with instantaneous peaks reaching nearly 42.4 A). This generates a neutral-to-phase loading factor of $k_N = 1.58$, placing the installation deep within the critical Red Zone. This scenario demonstrates that analytical calculations based solely on fundamental unbalance are insufficient, and dynamic BMS monitoring is mandatory to prevent immediate thermal failure when phases are unevenly loaded with non-linear equipment.

4.6. Synthesis of Results and Correlation with the BMS Decision

The effectiveness of the proposed algorithm for Smart Building management lies in its ability to interpret power quality indicators and generate corrective actions in real time. All data extracted from the four simulation scenarios (S0–S4) have been centralized in Table 6, which serves as a decision matrix for the automation system.

Table 6. Synthesis of performance indicators and system state according to the BMS logic.

Scenario	THD_i [%]	H_3 [%]	I_N (RMS) [A]	k_N	System State (BMS)	Management Action
S0	0%	0%	0	0	Green	Normal operation (Linear loads)

Table 6. *Cont.*

Scenario	THD_i [%]	H_3 [%]	I_N (RMS) [A]	k_N	System State (BMS)	Management Action
S1	0%	0%	3.5	0.35	Green	Monitoring (Minor unbalance)
S2	30%	30%	8.6	0.86	Yellow	Alert/Activate active filtering
S3	60%	60%	18.0	1.80	Red	Critical disconnection/Load isolation
S4	100%	100%	22.36	1.58	Critical—Red Zone	Emergency disconnection/Fire hazard prevention

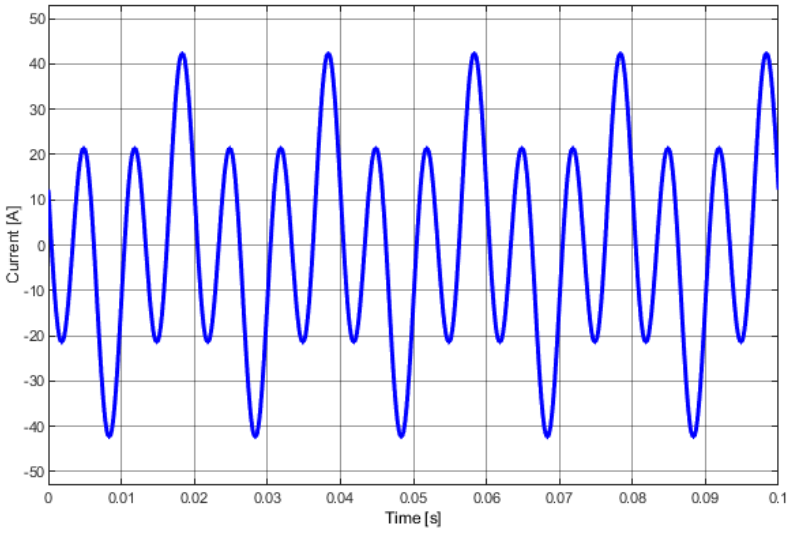

Figure 12. Oscillogram of the neutral conductor during Scenario S4 (extreme unbalance and harmonic pollution, Phase 3 disconnected). Note: The graph displays the voltage drop across the neutral equivalent resistance (R_N = 0.1 Ω); a peak value of ~4.24 V corresponds directly to an instantaneous peak current of ~42.4 A.

The analysis of the centralized data confirms the system's correct transition through the monitoring and protection states. In scenario S2, reaching the value of 8.6 A (k_N = 0.86) marks the BMS's automatic entry into the Yellow Zone, a decision strictly in accordance with the application of the thermal derating factor imposed by the international standard IEC 60364-5-52 for such a harmonic level [52].

By comparison, the evolution towards scenario S3 highlights the non-linear and accelerated nature of the stress applied to the neutral conductor. Although the harmonic content has doubled compared to S2, the neutral current has increased exponentially, reaching a critical value of 18 A (k_N = 1.80). This massive exceedance of the unitary threshold confirms that the neutral has become the most thermally stressed element in the network, placing the installation deep within the Red Zone and justifying radical protective intervention (load shedding) to prevent insulation degradation.

This correlation demonstrates that the k_N indicator is a significantly more precise predictor of thermal risk than the simple monitoring of the THD. Implementing the decision matrix within the BMS enables the proactive identification of thermal stress on the neutral conductor and the automatic triggering of protective measures before the infrastructure's integrity is compromised.

5. Discussion: Active Building Management

This section interprets the simulation results through the lens of real-world challenges in modern infrastructures, proposing a transition from traditional passive protection to an active and intelligent power quality management within Smart Buildings.

5.1. Interpretation of the "Neutral Shift" Phenomenon Under Balanced Conditions

The obtained results highlight a major paradox of electrical networks in modern buildings: the overloading of the neutral conductor under conditions of apparent phase load balance. In the classical theory of linear three-phase systems, equal phase currents cancel each other out, resulting in a zero neutral current.

However, as demonstrated by Scenario S3, the proliferation of electronic equipment (switched-mode power supplies, LED lighting, IT equipment) introduces a highly distorted mode. Zero-sequence harmonics, particularly those of the 3rd order (H_3) and multiples of 3, do not cancel out at the neutral node, but rather sum algebraically. This phenomenon leads to a "neutral shift" and the generation of a return current which, in our study, reached 180% of the nominal phase current value (I_N = 18 A compared to I_{ph} = 10 A). This massive accumulation is a direct consequence of the highly impulsive nature of the modeled SMPS loads, characterized by a severe crest factor of 1.89. The direct impact, previously validated through the analysis of Joule losses, is a thermal stress invisible to classical protection systems (circuit breakers calibrated solely for phase currents), which can lead to premature insulation degradation and major fire risks.

Furthermore, the introduction of the extreme test scenario (S4) demonstrates that analytical predictions based solely on fundamental unbalance are completely insufficient. When severe unbalance coincides with high harmonic pollution (e.g., Phase 3 disconnected, while Phases 1 and 2 supply highly distorted loads with $THDi$ = 100%), the neutral current experiences a massive arithmetic accumulation, reaching an extreme RMS value of 22.36 A (with instantaneous peaks of ~42.4 A) (k_N = 1.58). This worst-case scenario definitively proves that the neutral conductor can become the most vulnerable point of the infrastructure, reinforcing the absolute necessity for dynamic BMS monitoring rather than relying on static load distribution assumptions.

To ensure the correct design and reliable performance of the proposed BMS model, the accurate measurement and extraction of the third harmonic (and subsequent triplen harmonics) is critical. In practical Smart Building applications, this measurement is achieved using advanced Power Quality Analyzers (PQAs) or smart energy meters equipped with Digital Signal Processors (DSPs). These devices continuously sample the current waveforms and apply the FFT algorithm in strict accordance with the IEC 61000-4-7 standard [53]. The isolated harmonic data, including the precise magnitude of the third harmonic, is then transmitted to the BMS central controller via standard industrial protocols (e.g., Modbus RTU or BACnet). In our MATLAB/Simulink environment, this measurement process is accurately replicated using Discrete Fourier Transform (DFT) blocks, which extract the fundamental and harmonic components in real-time. The implications of this measurement accuracy are profound: the precise extraction of the third harmonic is the fundamental prerequisite for correctly calculating the k_N index. Any measurement error or processing delay would propagate directly into the BMS logical matrix, potentially causing false safety alarms or, more dangerously, failing to trigger derating protocols before the neutral conductor's thermal limits are exceeded.

5.2. Definition of the Automation Algorithm for Smart Buildings

The main novelty of this paper consists of translating the harmonic analysis into a decision-making tool applicable to BMS (Building Management System) environments.

Utilizing the neutral loading indicator (k_N) as an input variable for the logical control matrix enables the BMS to evaluate the "health" of the network in real-time and execute closed-loop actions.

A critical feature of the proposed BMS architecture is its dynamic adaptability to load changes. As the load profile of the building shifts from predominantly linear equipment to non-linear devices (such as IT infrastructure or EV chargers), the system's behavior changes significantly. The continuous monitoring of the k_N index allows the BMS to instantly detect this transition. While linear load variations keep the k_N index near zero, the introduction of non-linear single-phase loads causes k_N to rise dynamically, allowing the system to trigger safety protocols before critical thermal thresholds are breached.

Thus, under safe operating modes, the system performs exclusively passive data monitoring (data logging). As the proportion of non-linear loads increases and the installation enters the alert state, the BMS issues logistical alerts (Warnings) and can proactively command the activation of Active Power Filters (APF) to compensate for distortions before thermal stress accumulates.

The true value of the algorithm is demonstrated when critical neutral overload thresholds are reached. Upon exceeding extreme regulatory limits, the system no longer waits for the classical thermomagnetic protections to trip, but immediately initiates safety procedures:

- Load Shedding: The automatic and selective disconnection of non-essential circuits is executed as a last-resort measure to force a reduction in harmonic pollution levels. In a real-world BMS, load prioritization is predefined during the commissioning phase; "non-essential" loads refer to deferrable consumers (e.g., architectural facade lighting, common-area HVAC, secondary EV chargers), ensuring that the workstations, IT servers, and occupant productivity are not randomly disrupted.
- Isolation: To protect data integrity and critical processes, vital equipment is automatically transferred to double-conversion UPS (Uninterruptible Power Supply) sources.

By implementing this rule set, the installation's protection paradigm shifts. It is no longer purely reactive (waiting for a short-circuit or insulation melting), but becomes fundamentally proactive, focusing on overheating prevention and the building's energy optimization.

Furthermore, this software-based approach is highly cost-effective not only in native Smart Buildings, but especially in legacy buildings repurposed for modern IT infrastructure, where completely replacing undersized cables or installing large active filters is economically prohibitive.

5.3. Implications for Electrical Design and Predictive Maintenance

The conclusions of this study directly impact current electrical design standards. The traditional practice of undersizing the neutral conductor (using half the cross-section of the phase conductor) becomes a major safety risk in the IoT (Internet of Things) era. The results strongly suggest the necessity of oversizing the neutral conductor (to 1.5× or 2× the phase cross-section) in buildings characterized by a high density of electronic equipment.

However, relying solely on static design standards is often insufficient over a building's entire lifecycle due to the phenomenon of "load drift"—unpredictable changes in tenant equipment and harmonic pollution occurring years after the initial commissioning. Therefore, continuous software-based monitoring of the k_N parameter is essential to ensure that the physical limits established by these initial standards are not dynamically breached.

Furthermore, current sensors on the neutral conductor must become a mandatory standard within Smart Building architectures. The continuous monitoring of the total harmonic distortion ($THDi$) evolution and the H_3 component facilitates the transition

toward predictive maintenance. Instead of intervening after a cable or transformer failure, maintenance teams can utilize the historical BMS data (e.g., the gradual increase in the k_N parameter over several months) to identify insulation aging, inefficient load distribution across phases, or the need to recalibrate active harmonic filters. This approach ultimately optimizes operational costs while maximizing the building's overall safety.

6. Conclusions

This study analyzed the impact of non-linear loads on low-voltage electrical networks within Smart Buildings, highlighting the vulnerabilities of classical protection systems. Under conditions of a highly distorted mode ($THDi = 60\%$, $H_3 = 60\%$), triplen harmonics sum algebraically on the neutral conductor. The simulations demonstrated that under balanced highly distorted conditions, the neutral can reach a current up to 80% higher than the nominal phase current (18 A compared to 10 A). Moreover, under extreme operating conditions combining phase unbalance and severe harmonic pollution (Scenario S4), the neutral current surged to an extreme RMS value of 22.36 A (with instantaneous peaks reaching ~42.4 A), generating a critical loading factor of $k_N = 1.58$.

The analysis of Joule losses confirmed that this unbalance translates into critical thermal stress: the losses on the neutral conductor are more than three times higher than those on the phase conductor (peaks of approximately 65 W on the neutral vs. 20 W on the phase). This level of overload accelerates insulation degradation and represents an imminent fire risk.

To synthesize the findings, the data extracted from the simulated scenarios strictly validates the effectiveness of the proposed model for harmonic measurement and monitoring. By accurately capturing the 150 Hz zero-sequence components, the measurement architecture successfully translates the raw harmonic data into the dynamic k_N index. The direct correlation between the highly distorted simulation outputs—such as the massive neutral current reaching 180% (18 A) under balanced non-linear modes, and reaching an extreme RMS value of 22.36 A (with instantaneous peaks of ~42.4 A) under severe unbalance (S4), the non-zero neutral-to-ground voltage, and the quantified voltage distortion ($THD_V \approx 0.52\%$)—and the rapid response of the logical matrix demonstrates that the system is highly effective.

This direct link between the measured simulated data and the automated safety protocols proves the practical viability and diagnostic precision of the proposed BMS model, establishing a solid foundation for future physical implementations.

To prevent these risks, the proposed k_N parameter proved to be a robust indicator in evaluating power quality and preventing thermal risks. The threshold of $k_N \geq 0.86$ was identified for triggering the preventive alert state, while the value $k_N \geq 1.0$ (theoretical inflection point) defines the critical limit where the building management system (BMS) intervenes proactively. Integrating this decision matrix into the BMS logic enables the transition from passive to active protection. Through continuous monitoring, the system can trigger actions such as load shedding (disconnection of non-essential loads) or active filtering prior to the occurrence of a physical fault.

From the perspective of design recommendations, current standards require urgent revision for Smart Building infrastructures. It is imperatively recommended to abandon the practice of undersizing the neutral conductor in favor of its oversizing (1.5× or 2× the phase cross-section), to apply derating factors for transformers, and to mandatorily install current sensors on the neutral conductor.

Although the analysis validates the efficiency of the k_N index through rigorous numerical simulations, the study presents the inherent limitation of using a virtual environment (MATLAB/Simulink), focusing predominantly on the dominance of the 3rd-order harmonic

and partially neglecting external environmental factors. Therefore, future research will focus on two major directions. The first direction aims to develop an advanced thermodynamic model capable of translating electrical power losses directly into exact temperature variations (in degrees Celsius) at the cable insulation level. The second direction involves the experimental validation of the proposed algorithm (Hardware-in-the-Loop) on a real hardware architecture, utilizing physical cables and industrial IoT sensors within an operational infrastructure.

While this study successfully establishes the theoretical framework and simulative validation of the k_N index, future research will focus on the experimental validation of this automated BMS matrix on a physical, scaled-down Smart Building testbed, further analyzing the system's response under high-frequency load switching.

Furthermore, integrating such dynamic k_N-based monitoring systems paves the way for broader applications. This proactive approach aligns seamlessly with the latest research trends published in this journal, including advancements in passive harmonic filtration [54], coordinated harmonic compensation in microgrids [11], advanced profiling of harmonic sources [12], and the overarching transition toward positive energy districts in smart cities [55].

Author Contributions: Conceptualization, T.L., D.C.L. and D.P.; methodology, D.C.L. and G.B.; software, F.G.P. and A.M.T.; validation, D.C.L., D.P. and T.L.; formal analysis, D.I. and A.M.T.; investigation, D.C.L. and F.G.P.; resources, T.L. and G.B.; data curation, F.G.P. and G.B.; writing—original draft preparation, D.I. and D.P.; writing—review and editing, T.L., D.C.L. and D.P.; visualization, T.L., D.I. and D.C.L.; supervision, D.P., T.L. and F.G.P. All authors have read and agreed to the published version of the manuscript.

Funding: This research received no external funding.

Data Availability Statement: The original contributions presented in this study are included in the article. Further inquiries can be directed to the corresponding author.

Acknowledgments: The authors have reviewed and edited the output and take full responsibility for the content of this publication.

Conflicts of Interest: The authors declare no conflicts of interest.

Abbreviations

The following abbreviations are used in this manuscript:

APF	Active Power Filter
BMS	Building Management System
FFT	Fast Fourier Transform
H_3	3rd Harmonic Content (Ratio)
IEC	International Electrotechnical Commission
IT	Information Technology
k_N	Neutral-to-Phase Current Ratio
LED	Light-Emitting Diode
PVC	Polyvinyl Chloride
RMS	Root Mean Square
THDi	Total Harmonic Distortion of Current
UPS	Uninterruptible Power Supply
3P + N	Three-Phase and Neutral
SMPS	Switch-Mode Power Supplies
CF	Crest Factor

References

1. Espinosa Gutiérrez, J.S.; Aguila Téllez, A. Optimal Placement of a Unified Power Quality Conditioner (UPQC) in Distribution Systems Using Exhaustive Search to Improve Voltage Profiles and Harmonic Distortion. *Energies* **2025**, *18*, 4499. [CrossRef]
2. Cheepati, K.R.; Mariprasath, T.; Abarca, M.E.R.; Nageswara Rao, M. 1 Introduction to the Power Quality and Harmonic Power Filters. In *Designing Control Strategies for Harmonic Power Filters to Improve the Power Quality in Distribution Networks: Harmonic Power Filters Design*; River Publishers: Gistrup, Denmark, 2025; pp. 1–16. Available online: https://ieeexplore.ieee.org/document/10955962 (accessed on 21 March 2026).
3. Gaiceanu, M.; Epure, S.; Solea, R.C.; Buhosu, R. Power Quality Improvement with Three-Phase Shunt Active Power Filter Prototype Based on Harmonic Component Separation Method with Low-Pass Filter. *Energies* **2025**, *18*, 556. [CrossRef]
4. Chasi, C.; Velásquez, C.; Silva, B.; Espín, F.; Martínez-Gómez, J. Evaluation of Photometric and Electrical Parameters of LED Public Lighting for Energy Efficiency Compliance. *Energies* **2026**, *19*, 440. [CrossRef]
5. Zhou, X.; Chen, Q.; Zhang, L.; Wang, Q.; Zhou, N.; Peng, J.; Zhao, Y. A Unified Transformer-Based Harmonic Detection Network for Distorted Power Systems. *Energies* **2026**, *19*, 650. [CrossRef]
6. Koç, G.; Işık, Ö. The Effect of Temperature and Current on the Insulation Performance of PE and PVC Power Cables: A Finite Element Approach. *Energies* **2025**, *18*, 1366. [CrossRef]
7. Brenna, M.; Tironi, E.; Ubezio, G. Proposal of a Local DC Distribution Network with Distributed Energy Resources. In Proceedings of the 2004 11th International Conference on Harmonics and Quality of Power (IEEE Cat. No.04EX951), Lake Placid, NY, USA, 12–15 September 2004; pp. 397–402. Available online: https://ieeexplore.ieee.org/document/1409388 (accessed on 21 March 2026).
8. León-Martínez, V.; Montañana-Romeu, J.; Peñalvo-López, E.; León-Vinet, A.; Cano-Martínez, J. An Indirect Procedure for Real-Time Monitoring the Neutral Conductor Deterioration in Three-Phase Distribution Networks. *Machines* **2023**, *11*, 444. [CrossRef]
9. Pasculescu, D.; Pana, L.; Pasculescu, V.M.; Deliu, F. Economic criteria for optimizing the number and load factor of mining transformers. *Min. Miner. Depos.* **2019**, *13*, 1–16. [CrossRef]
10. Aslam, A.W.; Minambres-Marcos, V.; Roncero-Clemente, C. A Residential Droop-Controlled AC Nanogrid with Power Quality Enhancement. *Electronics* **2025**, *14*, 3306. [CrossRef]
11. Zobaa, A.F. Mixed-integer distributed ant colony multi-objective optimization of single-tuned passive harmonic filter parameters. *IEEE Access* **2019**, *7*, 44862–44870. [CrossRef]
12. Ma, H.; Girgis, A.A. Identification and tracking of harmonic sources in a power system using a Kalman filter. *IEEE Trans. Power Deliv.* **1996**, *11*, 1659–1665. [CrossRef]
13. Alawasa, K.; Al-Odienat, A. Power Quality Investigation of Single Phase Grid-connected Inverter of Photovoltaic System. *J. Eng. Technol. Sci.* **2019**, *51*, 597–614. [CrossRef]
14. Pasculescu, V.M.; Radu, S.M.; Pasculescu, D.; Niculescu, T. Dimensioning the intrinsic safety barriers of electrical equipment intended to be used in potentially explosive atmospheres using the SimPowerSystems software package. *Int. Multidiscip. Sci. GeoConf. SGEM* **2013**, *1*, 417. [CrossRef]
15. Spunei, E.; Frumușanu, N.-M.; Martin, M. Study on Household-Level Electricity Consumption of Domestic Consumers in Romania: The Need to Check the Electrical Installation. *Sustainability* **2024**, *16*, 4203. [CrossRef]
16. Pechlivanis, C.; Rigogiannis, N.; Tichalas, A.; Frantzeskakis, S.; Christodoulou, C.; Papanikolaou, N. Active Fault Detection Device for LV Electrical Installations with Goertzel-Based Impedance Estimation and IoT Connectivity. *Eng. Proc.* **2024**, *60*, 22. [CrossRef]
17. Tawalbeh, M.; Al-Othman, A.; Kafiah, F.; Abdelsalam, E.; Almomani, F.; Alkasrawi, M. Environmental impacts of solar photovoltaic systems: A critical review of recent progress and future outlook. *Sci. Total Environ.* **2021**, *759*, 143528. [CrossRef]
18. Pessoa, A.L.d.S.; Oleskovicz, M.; Martins, P.E.T. A Multi-Stage Methodology for Fault Location in Radial Distribution Systems. In Proceedings of the 2018 18th International Conference on Harmonics and Quality of Power (ICHQP), Ljubljana, Slovenia, 13–16 May 2018; pp. 1–6. Available online: https://ieeexplore.ieee.org/document/8378852 (accessed on 22 March 2026).
19. Rakov, V.A.; Uman, M.A.; Fernandez, M.I.; Mata, C.T.; Rambo, K.J.; Stapleton, M.V.; Sutil, R.R. Direct Lightning Strikes to the Lightning Protective System of a Residential Building: Triggered-Lightning Experiments. *IEEE Trans. Power Deliv.* **2002**, *17*, 575–586. [CrossRef]
20. Kelm, P.; Mieński, R.; Wasiak, I. Energy Management in a Prosumer Installation Using Hybrid Systems Combining EV and Stationary Storages and Renewable Power Sources. *Appl. Sci.* **2021**, *11*, 5003. [CrossRef]
21. Dumitrescu, M. Isolated Power System Safety Analysis. *Proceedings* **2020**, *63*, 21. [CrossRef]
22. Parol, M.; Stepaniuk, M. The Installations and Systems in Intelligent Buildings as an Element of Smart Cities Concept. In Proceedings of the 2018 15th International Conference on the European Energy Market (EEM), Lodz, Poland, 27–29 June 2018; pp. 1–5. Available online: https://ieeexplore.ieee.org/document/8469887 (accessed on 22 March 2026).

23. Oncioiu, I.; Man, M.; Pirvu, C.A.L.; Hojda, M.H. A Data-Driven Zonal Monitoring Framework Based on Renewable Variability for Power Quality Management in Smart Grids. *Sustainability* **2025**, *17*, 7737. [CrossRef]
24. Carní, D.L.; Lamonaca, F. Local Distributed Node for Power Quality Event Detection Based on Multi-Sine Fitting Algorithm. *Sensors* **2024**, *24*, 2474. [CrossRef]
25. Liubčuk, V.; Radziukynas, V.; Kairaitis, G.; Naujokaitis, D. Power Quality Monitors Displacement Based on Voltage Sags Propagation Mechanism and Grid Reliability Indexes. *Appl. Sci.* **2023**, *13*, 11778. [CrossRef]
26. Barukin, A.; Berguzinov, A.; Talipov, O. Mounting Measuring Devices of Reed Switch Protection Near Conductors of Electrical Installations. In Proceedings of the 2020 International Multi-Conference on Industrial Engineering and Modern Technologies (FarEastCon), Vladivostok, Russia, 6–9 October 2020; pp. 1–6. Available online: https://ieeexplore.ieee.org/document/9271569 (accessed on 22 March 2026).
27. Pana, L.; Grabara, J.; Moraru, R.I.; Pasculescu, D.; Pasculescu, V.M. Optimal quality management algorithm for assessing the usage capacity level of mining transformers. *Pol. J. Manag. Stud.* **2018**, *18*, 233–244. [CrossRef]
28. Ildarabadi, R.; Zadehbagheri, M. New Technology and Method for Monitoring the Status of Power Systems to Improve Power Quality—A Case Study. *Processes* **2023**, *11*, 2468. [CrossRef]
29. Liubčuk, V.; Radziukynas, V.; Naujokaitis, D.; Kairaitis, G. Grid Nodes Selection Strategies for Power Quality Monitoring. *Appl. Sci.* **2023**, *13*, 6048. [CrossRef]
30. Mohammed, M.; Riad, K.; Alqahtani, N. Design of a Smart IoT-Based Control System for Remotely Managing Cold Storage Facilities. *Sensors* **2022**, *22*, 4680. [CrossRef]
31. Hernández, J.C. Grid-Connected Renewable Energy Sources. *Electronics* **2021**, *10*, 588. [CrossRef]
32. Sagar; Singhal, P.; Arya, Y. Building Energy Management System for the Demand Response of a Residential Green Building Based on Optimization Technique. In Proceedings of the 2024 2nd International Conference on Cyber Physical Systems, Power Electronics and Electric Vehicles (ICPEEV), Hyderabad, India, 26–28 September 2024; pp. 1–6. Available online: https://ieeexplore.ieee.org/document/10931939 (accessed on 21 March 2026).
33. Cao, Y.; Zhang, Y.; Wen, T.; Li, P. Research on dynamic nonlinear input prediction of fault diagnosis based on fractional differential operator equation in high-speed train control system. *Chaos* **2019**, *29*, 013130. [CrossRef]
34. Krishnamurthy, N.K.; Sabhahit, J.N.; Jadoun, V.K.; Pandey, A.K.; Rao, V.S.; Saraswat, A. A Grid-Interfaced DC Microgrid-Enabled Charging Infrastructure for Empowering Smart Sustainable Cities and Its Impacts on the Electrical Network: An Inclusive Review. *Smart Cities* **2025**, *8*, 176. [CrossRef]
35. Viciana, E.; Alcayde, A.; Montoya, F.G.; Baños, R.; Arrabal-Campos, F.M.; Zapata-Sierra, A.; Manzano-Agugliaro, F. OpenZmeter: An Efficient Low-Cost Energy Smart Meter and Power Quality Analyzer. *Sustainability* **2018**, *10*, 4038. [CrossRef]
36. Hajiabadi, H.; Zafari, M. Energy Efficiency and Pollution Reduction Through Intelligent Building Management Systems. In Proceedings of the 2025 33rd International Conference on Electrical Engineering (ICEE), Isfahan, Islamic Republic of Iran, 13–15 May 2025; pp. 769–774. Available online: https://ieeexplore.ieee.org/document/11213620 (accessed on 22 March 2026).
37. Lazar, D.C.; Petrilean, D.C.; Lazar, T.; Popescu, F.G.; Ionescu, D.; Tatar, A.M.; Buica, G.; Pasculescu, D. Real-Time Energy System Optimization and Resilience Analysis in Low-Voltage Networks Using Intelligent Edge Computing. *Processes* **2026**, *14*, 660. [CrossRef]
38. Dekhandji, F.Z.; Recioui, A.; Ladada, A.; Moulay Brahim, T.S. Detection and Classification of Power Quality Disturbances Using LSTM. *Eng. Proc.* **2023**, *29*, 2. [CrossRef]
39. Moreno-Garcia, I.M.; Palacios-Garcia, E.J.; Pallares-Lopez, V.; Santiago, I.; Gonzalez-Redondo, M.J.; Varo-Martinez, M.; Real-Calvo, R.J. Real-Time Monitoring System for a Utility-Scale Photovoltaic Power Plant. *Sensors* **2016**, *16*, 770. [CrossRef] [PubMed]
40. Li, W.; Logenthiran, T.; Phan, V.-T.; Woo, W.L. Intelligent Housing Development Building Management System (HDBMS) for Optimized Electricity Bills. In Proceedings of the 2017 IEEE International Conference on Environment and Electrical Engineering and 2017 IEEE Industrial and Commercial Power Systems Europe (EEEIC/I&CPS Europe), Milan, Italy, 6–9 June 2017; pp. 1–6. Available online: https://ieeexplore.ieee.org/document/7977410 (accessed on 22 March 2026).
41. Xu, T.; Aini, A.M.; Nordin, N.A.; Shen, Q.; Huang, L.; Xu, W. Symbiotic Intelligence for Sustainable Cities: A Decadal Review of Generative AI, Ethical Algorithms, and Global South Innovations in Urban Green Space Research. *Buildings* **2026**, *16*, 231. [CrossRef]
42. Ahmad, A.M.; Abdelkarim, S.B.; Adalbi, M.; Elnahhas, R.; Naji, K. Developing Critical Success Factors (CSF) for Integrating Building Information Models (BIM) into Facility Management Systems (FMS). *Buildings* **2025**, *15*, 3434. [CrossRef]
43. Salam, S.M.; Uddin, M.J.; Hannan, S. A New Approach to Develop a Template Based Load Model that can Dynamically Adopt Different Types of Non-Linear Loads. In Proceedings of the 2017 International Conference on Electrical, Computer and Communication Engineering (ECCE), Cox's Bazar, Bangladesh, 16–18 February 2017; pp. 708–712. Available online: https://ieeexplore.ieee.org/document/7912996 (accessed on 22 March 2026).
44. Pasculescu, D.; Riurean, S.; Ilieva-Obretenova, M.; Lazar, T.; Tatar, A.M.; Fita, N.D. Intelligent Modeling of PV–BESS Microgrids for Enhanced Stability, Cyber–Physical Resilience and Blackout Prevention. *Energies* **2026**, *19*, 148. [CrossRef]

45. Alam, S.M.M.; Ali, M.H. An Overview of State-of-the-Art Research on Smart Building Systems. *Electronics* **2025**, *14*, 2602. [CrossRef]
46. Su, W.; Li, Z.; Shao, Z. The Harmonic Calculation Model of Non-Linear Load. In Proceedings of the 2014 China International Conference on Electricity Distribution (CICED), Shenzhen, China, 23–26 September 2014; pp. 866–872. Available online: https://ieeexplore.ieee.org/document/6991832 (accessed on 22 March 2026).
47. Khan, T.A.; Kahwash, F.; Ahmed, J.; Goh, K.; Papadopoulos, S. From Design to Deployment: A Comprehensive Review of Theoretical and Experimental Studies of Multi-Energy Systems for Residential Applications. *Electronics* **2025**, *14*, 2221. [CrossRef]
48. Vandenbogaerde, L.; Verbeke, S.; Audenaert, A. Optimizing building energy consumption in office buildings: A review of building automation and control systems and factors influencing energy savings. *J. Build. Eng.* **2023**, *76*, 107233. [CrossRef]
49. Marcu, M.D.; Popescu, F.G.; Niculescu, T.; Pana, L.; Handra, A.D. Simulation of Power Active Filter Using Instantaneous Reactive Power Theory. In Proceedings of the 2014 IEEE 16th International Conference on Harmonics and Quality of Power (ICHQP), Bucharest, Romania, 25–28 May 2014; pp. 581–585. [CrossRef]
50. Dietmannsberger, M.; Schulz, D. Different Load Types and Their Effect on Islanding Detection and Control in Low Voltage Grids. In Proceedings of the 2016 10th International Conference on Compatibility, Power Electronics and Power Engineering (CPE-POWERENG), Bydgoszcz, Poland, 29 June–1 July 2016; pp. 222–227. Available online: https://ieeexplore.ieee.org/document/7544189 (accessed on 22 March 2026).
51. Marcu, M.D.; Popescu, F.G.; Pana, L. Modeling and simulation of power active filters for reducing harmonic pollution using the instantaneous reactive power theory. *Environ. Eng. Manag. J.* **2014**, *13*, 1377–1382. Available online: https://eemj.eu/index.php/EEMJ/article/view/1951 (accessed on 22 March 2026). [CrossRef]
52. *IEC 60364-5-52*; Low-Voltage Electrical Installations—Part 5-52: Selection and Erection of Electrical Equipment—Wiring Systems. International Electrotechnical Commission: Geneva, Switzerland, 2009.
53. *IEC 61000-4-7*; Electromagnetic Compatibility (EMC)—Part 4-7: Testing and Measurement Techniques—General Guide on Harmonics and Interharmonics Measurements and Instrumentation, for Power Supply Systems and Equipment Connected Thereto. International Electrotechnical Commission: Geneva, Switzerland, 2002.
54. Eroğlu, H.; Cuce, E.; Cuce, P.M.; Gul, F.; Iskenderoğlu, A. Harmonic problems in renewable and sustainable energy systems: A comprehensive review. *Sustain. Energy Technol. Assess.* **2021**, *48*, 101566. [CrossRef]
55. Tuerk, A.; Frieden, D.; Neumann, C.; Latanis, K.; Tsitsanis, A.; Kousouris, S.; Llorente, J.; Heimonen, I.; Reda, F.; Ala-Juusela, M.; et al. Integrating Plus Energy Buildings and Districts with the EU Energy Community Framework: Regulatory Opportunities, Barriers and Technological Solutions. *Buildings* **2021**, *11*, 468. [CrossRef]

Disclaimer/Publisher's Note: The statements, opinions and data contained in all publications are solely those of the individual author(s) and contributor(s) and not of MDPI and/or the editor(s). MDPI and/or the editor(s) disclaim responsibility for any injury to people or property resulting from any ideas, methods, instructions or products referred to in the content.